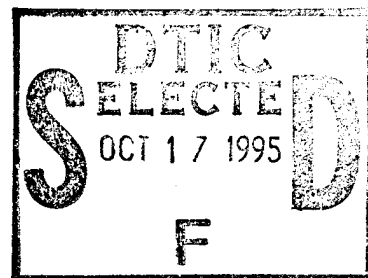# FINAL REPORT

STRUCTURAL AND MAGNETIC CHARACTERIZATION OF Fe_xCo_{1-x} ALLOY FILM STRUCTURES

A
PROJECT
IN RESPONSE TO

OCNRINST 3912.1
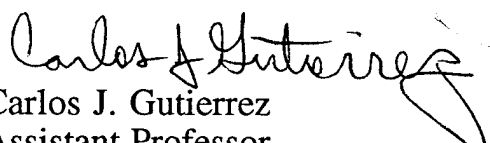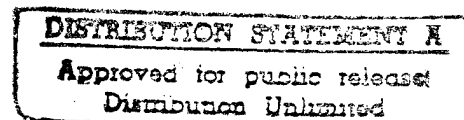
NRC-NRL RESEARCH ASSOCIATE POST-TENURE
INSTRUMENTATION PROGRAM

PI: Carlos J. Gutierrez
     Assistant Professor
     Department of Physics
     Southwest Texas State University
     San Marcos, TX 78666
     (512) 245-3647 or 2131, and 8095 (FAX)
     e-mail: CG08@ACADEMIA.SWT.EDU

Applicable Topic Areas:
1) Ultra-thin magnetic films
2) Novel phases / artificially-structured materials
3) Magneto-transport

19951012 072

FINAL PROJECT REPORT

This project originally focused on the synthesis and characterization of MBE-grown FeCo alloy magnetic film structures. This emphasis was carried through successfully, however, additional related project components dealing with sputtered permalloy and cobalt films were also conducted. The decision to include these new materials kept within the focus of establishing a successful new research initiative investigating novel magnetic film phenomena with an accent towards possible implementation in magnetic film device applications (including giant magnetoresistance).

As projected in the original proposal, additional synthesis and characterization of epitaxial FeCo alloy film structures on ZnSe-buffered GaAs(001) substrates was conducted using MBE facilities available at the Naval Research Lab (NRL). The major accomplishment was the synthesis of epitaxial $Fe_{25}Co_{75}/Mn/Fe_{25}Co_{75}(001)$ trilayers with varying Mn thicknesses. The composition of the $Fe_{25}Co_{75}(001)$ alloy films were chosen to lie on the edge of thermodynamic stability for the bcc (body centered cubic) crystal structure. In this way, the excellent film growth characteristics (smooth interfaces, high-quality single-crystalline perfection) of the bcc Co-rich alloys was used to induce a subsequently grown metastable bct (body centered tetragonal) Mn(001) film structure which was characterized *in-situ* by RHEED. Furthermore, it was also found from RHEED that the regrowth of a second $Fe_{25}Co_{75}(001)$ film on the finished metastable bct Mn also yielded excellent bcc film quality. In this way, a robust configuration of bct Mn could be trapped between two high-quality bcc $Fe_{25}Co_{75}(001)$ films.

Although PI's involvement in the successful synthesis of bct Mn(001) thin films was an achievement in itself, the magnetic characteristics of this $Fe_{25}Co_{75}/Mn$ system proved even more fascinating. The resulting hysteresis loops for the thickest Mn films indicated that the FeCo layers were acting almost independently of one another. However, thinner Mn layers (< 3 nm) resulted in trilayer loops with features indicative of strong 90 degree (biquadratic coupling). The analysis of these hysteresis loops required careful SQUID and FMR analysis conducted by collaborators (Filipkowski, Krebs) at NRL. These time-consuming measurements were needed to untangle the effects of four-fold and uniaxial magnetic anisotropy in the $Fe_{25}Co_{75}(001)$ alloy layers from the effects of the strong biquadratic coupling contribution. Over the complete range of Mn intermediate layers that were synthesized in the series, evidence for significant 180 degree (bilinear coupling) was never observed. Furthermore, it was found that the biquadratic term for this Mn system had a slight temperature dependence, an observation in sharp contrast with the epitaxial Fe/Al system. Indeed, this project was slowed because of a lack of a valid theoretical model

explaining the magnetic characteristics for this system. However, this work on the $Fe_{25}Co_{75}$/Mn system prompted Dr. John Slonczewski to develop a model (submitted to *J. Magn. Magn. Mat.*) based upon trilayer systems where an ordered antiferromagnetic layer is placed between two ferromagnetic layers. This phase of the project led to a manuscript (enclosed) which is currently being refereed for acceptance in *Physical Review Letters*. In addition, the PI's conception and synthesis of these FeCo/Mn trilayers has resulted in an ongoing collaborative investigation involving the Brookhaven NSLS and the Missouri University Research Reactor (MURR). Collaborative investigations with Idzerda, *et al.*, has yielded EXAFS measurements that confirm the bct structure of the metastable Mn layers trapped in these trilayers. Furthermore, SXMCD measurements confirm the 90 coupling between the $Fe_{25}Co_{75}$ layers for $t_{Mn} < 3$ nm inferred from the complex hysteresis loops, and the observation of a Mn moment has been observed (preprint manuscript enclosed, submitted to *Physical Review Letters*). More recently, neutron reflectivity measurements have also confirmed the existence of the 90 degree coupling in these trilayers (work is ongoing).

The very interesting behavior of these FeCo/Mn trilayers synthesized by the PI has placed these samples in great demand for characterization. Subsequently, it has been impossible to find a satisfactory window of opportunity for glancing x-ray measurements using the Bede 200 system at SWT. However, the x-ray system purchased in part by this ONR grant has been installed at SWT. Double-crystal and glancing incidence measurements of standard epitaxial SiGe films have been performed subsequent to installation, revealing a defect in the silicon channel-cut collimator (CCC) used for beam compression and monochromatization which results in unnecessary line-width broadening. A replacement component CCC is being constructed for installation in June 95. Negotiations for FeCo/Mn sample transfer from NRL to SWT for the x-ray reflectivity and rocking curve measurements have determined that the trilayer samples will be available for analysis by the PI at SWT soon after the x-ray system servicing. It is expected that these x-ray measurements will lend further information regarding average interfacial roughness. Later, these will be compared to four-point probe magnetotransport measurements of the trilayers.

The analysis capability of the Bede 200 x-ray system in connection with the unexpected acquisition of a dual ion beam sputtering system by the PI at SWT has led to a related opportunity to initiate an investigation of permalloy-based polycrystalline magnetic multilayers (chiefly their hysteresis and magnetotransport properties). In addition, an available DC magnetron sputtering system was extensively reconfigured for Co-based multilayer growths at SWT from 1/94 to 10/94. Prompted by Hylton et al.'s work on annealed discontinuous permalloy-silver multilayers, the PI decided to conduct a similar investigation on annealed Co/Cu multilayers. Using a 96% Ar and 4%

H_2 mixture for the sputtering gas operating at 10 millitorr, a complete series of Co/Cu multilayers (15 or 30 repeat cycles) with $t_{Co} = 2.5$ nm and 2 nm $< t_{Cu} < 4$ nm were synthesized at SWT on buffered oxidized (~20 nm SiO_2) silicon substrates held ~room temperature. Film thicknesses were obtained at SWT from stylus profilometry calibrated sputter deposition rates, and later spot checked with EDAX measurements. The as-grown (not annealed) VSM hysteresis loops measured at SWT yielded relatively simple "S-like" hysteresis loops with typical coercivities ranging from 50 - 70 Oe (a typical example is shown in the attached supplement summarizing Co/Cu work). Later, similarly grown Co/Cu films were synthesized and annealed for 30 minutes at either 350°C or 450°C in a 96% Ar and 4% H_2 mixture held at 10 millitorr. There was an in-plane ~500 Oe magnetic field acting on the film during the annealing process. The annealing produced more complex VSM hysteresis loops with "double-waisted" characteristics and enlarged coercivities (typically 70 - 110 Oe). It is suspected that the more complex hysteresis is the result of an anneal-induced preferential grain-growth process establishing two slightly different average grain size distributions with slightly different coercivities. However, this conjecture will be tested by scheduled Bede 200 system x-ray diffraction and reflectivity measurements in summer 1995.

Besides the increase in coercivity, the annealing process increased the observed CIP GMR as defined by $(R_{max} - R_{min})/R_{min} = $ GMR from a typical value of 1.6% - 3% for the unannealed multilayers to 3.1% - 5.5% for the annealed multilayers. The GMR measurements were conducted in collaboration with Dr. Martin Sablik at Southwest Research Institute. This Co/Cu work was reported by SWT masters degree graduate student Luis Tristan at the January 1995 SACNAS (Society for the Advancement of Chicanos and Native Americans in Science) National Conference held in El Paso, and by SWT masters degree graduate student Robert Dail at the March 1995 Meeting of the Texas Section of the American Physical Society (xeroxes of the transparencies used for the APS meeting are submitted). This work is only preliminary, indeed the spread of coercivities in the Co/Cu multilayers indicate that run-to-run variations need to be minimized. The most likely culprit for these variations is the need for a more precise control of pressure, which is now being addressed. In summer 1995, the Co/Cu work will be more carefully repeated, followed by work utilizing $Co_{90}Fe_{10}$/Cu multilayer films utilizing a low magnetostriction $Co_{90}Fe_{10}$ alloy susceptible to the magnetic annealing effect. The results of this combined work will be submitted for publication.

Lastly, the effects of dual ion beam processing parameters on polycrystalline permalloy films synthesized on oxidized silicon was initiated. This work was done in collaboration with Dr. Steve Michel at Commonwealth Scientific. Before multilayers using permalloy could be constructed, it was necessary to understand the behavior of single layer permalloy films. A series of permalloy

films with 20 nm < t < 50 nm were deposited at various target sputter gun energies, and with or without the presence of a second ion beam assist gun (100 eV) impinging on the growing film surface. Furthermore, an in-plane ~150 Oe magnetic field was allowed to act on the growing film held at room temperature. In all cases, the magnetic field present during growth acted to create a uniaxial anisotropy (typically ~ 5 Oe) with the easy axis parallel to the direction of the applied magnetic field during growth. VSM measurements conducted at SWT indicated that for 500 eV target gun energy, the permalloy films grown without ion beam assist exhibited ~1 Oe of coercivity, while the same conditions with the presence of 100 eV ion beam assist during film growth increased the coercivity to ~1.5 Oe. This uniaxial anisotropy and influence of ion beam assist on coercive properties can be seen in the hysteresis figures shown in the accompanying supplement with a detailed description of the dual gun ion beam project. Additional MR and x-ray analysis work at SWT is planned for Summer 95. The motivation for investigating these differences in ion beam sputtered permalloy is for the possibility of constructing a spin valve structure with low coercivity properties. For example, in principle, an attractive spin valve multilayer constructed from permalloy and copper can be constructed using low-coercivity permalloy (without ion beam assist treatment) / copper / high-coercivity permalloy (with ion beam assist treatment). Preliminary results indicate that this type of spin-valve structure is indeed possible - a 30 cycle multilayer with 2.5 nm thick permalloy layers and 4 nm thick Cu layers utilizing this ion beam process degree of freedom has been successfully constructed (see the last figure in the accompanying supplement with a detailed description of the dual gun ion beam project). Follow-up work for GMR, FMR, and neutron reflectivity measurements are being planned. Preliminary results from this research effort have been presented by SWT masters degree graduate student Luis Tristan at the March 1995 Meeting of the Texas Section of the American Physical Society (xeroxes of the transparencies used for the APS meeting are submitted). A more complete treatment will be submitted for the upcoming 1995 MMM Conference.

In conclusion, this ONR project has indeed accomplished the goal of providing the PI with initial start-up for research within a university setting. In May 1995, the PI was named a CAREER (formerly called "Young Investigator") grant recipient by the NSF for magnetic film research. The availability of a Bede 200 x-ray system for thin film analysis has helped the PI leverage the acquisition of a versatile dual gun ion beam sputtering system and 3-source DC magnetron system for magnetic film analysis. Furthermore, the availability of VSM, SEM/EDS, and magnetotransport apparatus for magnetic film analysis has been assisted by this ONR project. Lastly, this ONR project has contributed towards the research training of three SWT undergraduates, and four SWT masters degree students. Of these, Mr. Marwan Khater and Mr. Luis Tristan have completed their thesis work.

SWT STUDENTS IMPACTED BY THE PROJECT:

A. Undergraduates (*Mexican-American)
   1. *Mr. Anival Ayala
   2. *Mr. Raymond Selestino
   3. Mr. Brian Woodchek

B. Masters Degree Students (*Mexican-American)
   1. Mr. Robert Dail ("X-ray Characterization of Layered Magnetic Multilayers", ~5/96)
   2. Mr. Marwan Khater ("Sputtered FeCo and Permalloy Magnetic Films", 8/94) (presently a PhD candidate at the Physics Dept. at the Univ. of Texas at Dallas)
   3. *Mr. David Medrano ("The Antimicrobial Activity of Sputtered Metallic Films", ~5/96)
   4. *Mr. Luis Tristan ("Synthesis of Sputtered Co/Cu GMR Film Structures", 5/95) (offered employment by Applied Materials)

MEETINGS ATTENDED:

(1)   1993 MMM CONFERENCE
(2)   1994 JOINT MMM-INTERMAG CONFERENCE
(3)   1994 APS CONFERENCE (MARCH MEETING)
(4)   1995 INTERMAG CONFERENCE
(5)   1994 TEXAS SECTION OF THE APS
(6)   1995 TEXAS SECTION OF THE APS

PENDING MANUSCRIPTS:

(1)   *GIANT NEAR-90 DEGREE COUPLING IN EPITAXIAL FeCo/Mn/FeCo SANDWICH STRUCTURES*, with M.E. Filipkowski, J.J. Krebs, and G.A. Prinz (submitted to *Phys. Rev. Lett.* in 1995)
(2)   *MAGNETIC CIRCULAR DICHROISM STUDIES OF FeCo/Mn/FeCo*, WITH V. Chakarian, H.J. Lin, Y.U. Idzerda, E.E. Chaban, G. Meigs, J.H. Park, G.A. Prinz, and C.T. Chen (submitted to *Phys. Rev. Lett.* in 1995)

RECENT SWT PRESENTATIONS:

(1) "Coercivity Modifications in Soft Permalloy Films Synthesized by Dual Ion Beam Sputtering", with L. Tristan, R. Dail, M. Khater, and D. Medrano (submitted to Texas Section APS Spring 95 Meeting)

(2) "Synthesis and Characterization of Annealed Co/Cu Multilayer Thin Films", with L. Tristan, R. Dail, M. Khater, D. Medrano, D. Stead, and M.J. Sablik (submitted to Texas Section APS Spring 95 Meeting)

PROJECT BUDGET

RESOURCES:

AMOUNT REQUESTED FROM ONR:	$50,000
SWT MATCHING GRANT (CAPITAL EQUIPMENT):	$50,000
SWT START-UP FUNDS:	$25,000
SWT RESEARCH ENHANCEMENT GRANT FUNDS:	$5,910
TOTAL FUNDS AVAILABLE:	$130,910

EXPENSES:

ALLOCATION FOR NON-EXPENDIBLE EQUIPMENT:	$125,370 (*)

(*) Consisting of:

Bede 200 Double Crystal Diffractometer System	$70,470
3 K.W. x-ray generator	$39,900
x-ray reflectivity simulation software	$2,500
x-ray alignment imaging device	$7,750
beam compression crystal	$1,750
installation	$3,000

ALLOCATION FOR EXPENDIBLE EQUIPMENT:	$5,540
ALLOCATION FOR SALARY SUPPORT:	$0
TOTAL:	$130,910

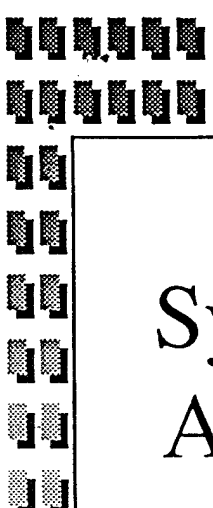($50,000 from ONR and $80,910 from SWT)
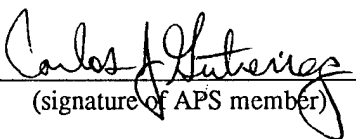
Magnetic Films

Synthesis and Characterization of Annealed Co/Cu Multilayer Thin Films,
R. Dail, L. Tristan, M. Khater, D. Medrano; Dr. C. J. Gutierrez, Physics Dept.,
Southwest Texas State University and Dr. M. J. Sablik, D. Stead, Southwest
Research Institute.-- Multilayers were produced by DC Magnetron Sputtering in a
high-vacuum chamber. An ultrahigh purity gas mixture of Ar (96%) and H_2 (4%)
was used as the sputtering gas. After growth, some of the multilayers were
annealed in a magnetic field in an effort to modify magnetic anisotropy and
coercivity. Multilayer component thicknesses ranged from 5 Å to 25 Å for Co, and
5 Å to 50 Å for Cu. Thickness calibrations were obtained by stylus profilometry
(Tencor Alpha-Step 200), and spot-checked using a SEM equipped with an EDAX
detector. Multilayers of 15 and 30 bilayer periods were produced and deposited
onto oxidized silicon substrates, and hysteresis loops were obtained using a
Vibrating Sample Magnetometer. GMR measurements were made with a four-
point linear probe with in-plane magnetic fields. Samples produced have exhibited
a GMR of ~5%.

(signature of APS member)

Prefer Standard Session

Carlos J. Gutierrez
Dept. of Physics
Southwest Texas State University
San Marcos, TX 78666
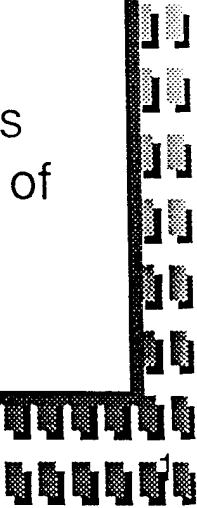(512) 245-2131, 245-8233 (FAX)
CG08@ACADEMIA.SWT.EDU

Synthesis and Characterization of Annealed Co/Cu Multilayer Thin Films

Robert Dail, B.S.
Southwest Texas State University

Marwan Khater

Luis Tristan

David Medrano

Dr. Carlos J. Gutierrez, Professor

Dr. Martin J. Sablik, Staff Scientist

D. Stead, Engineer

Southwest Research Institute

Synthesis

- **Substrate Preparation**
  - 1.5 cm^2 Si wafers with ~200 SiO$_2$
  - Chemical rinse
  - Blow-dry with ultra-high purity N$_2$
- **Film growth**
  - Substrates were mounted on heater for *in situ* anneal
  - DC Magnetron sputtered
- **Anneal**
  - Films were annealed in a magnetic field
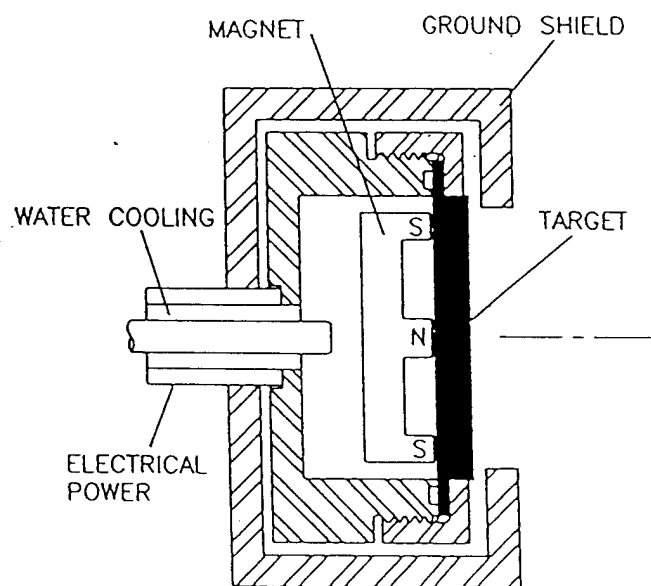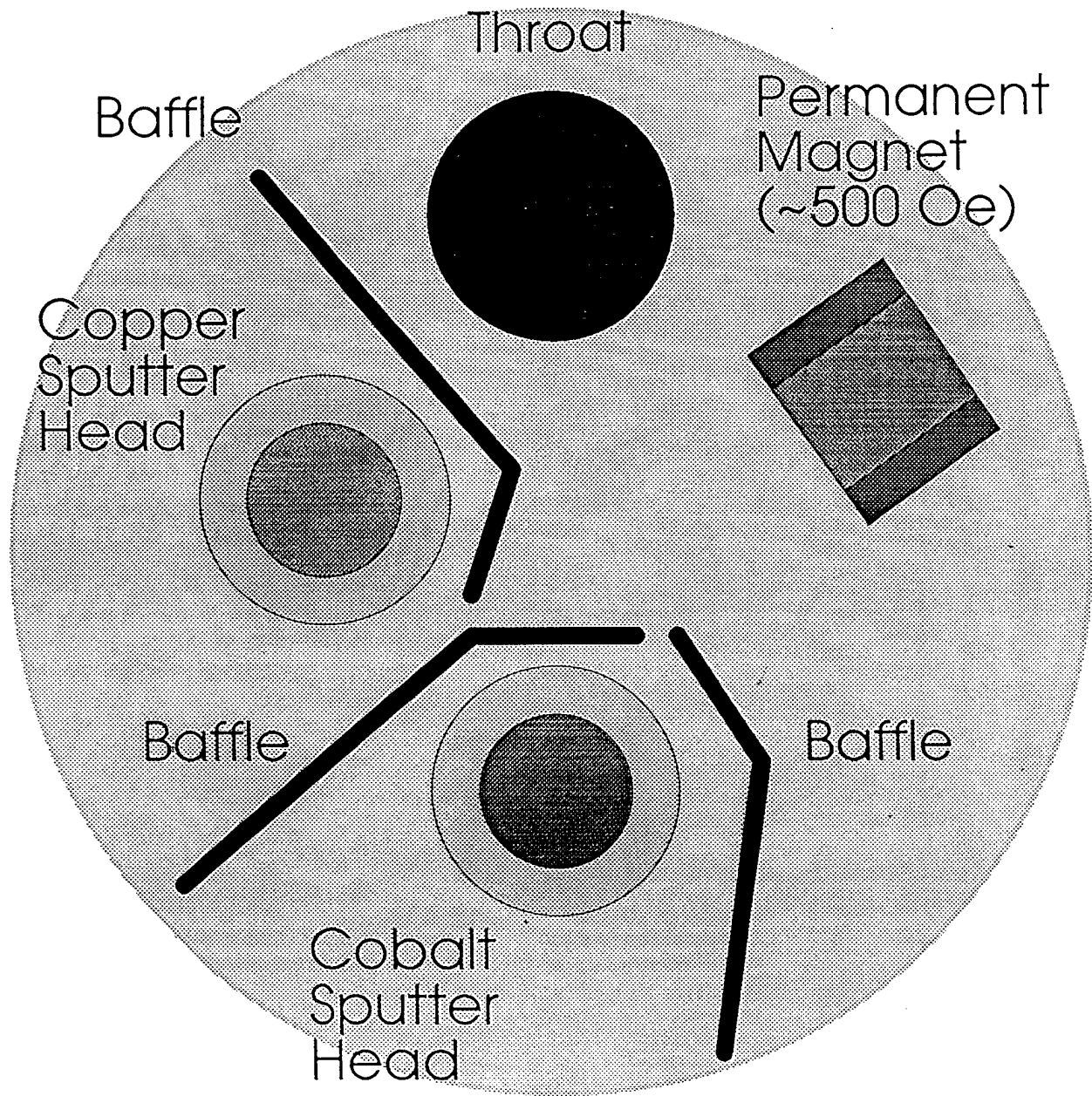 - 30 minute anneal at 350°C and 450°C
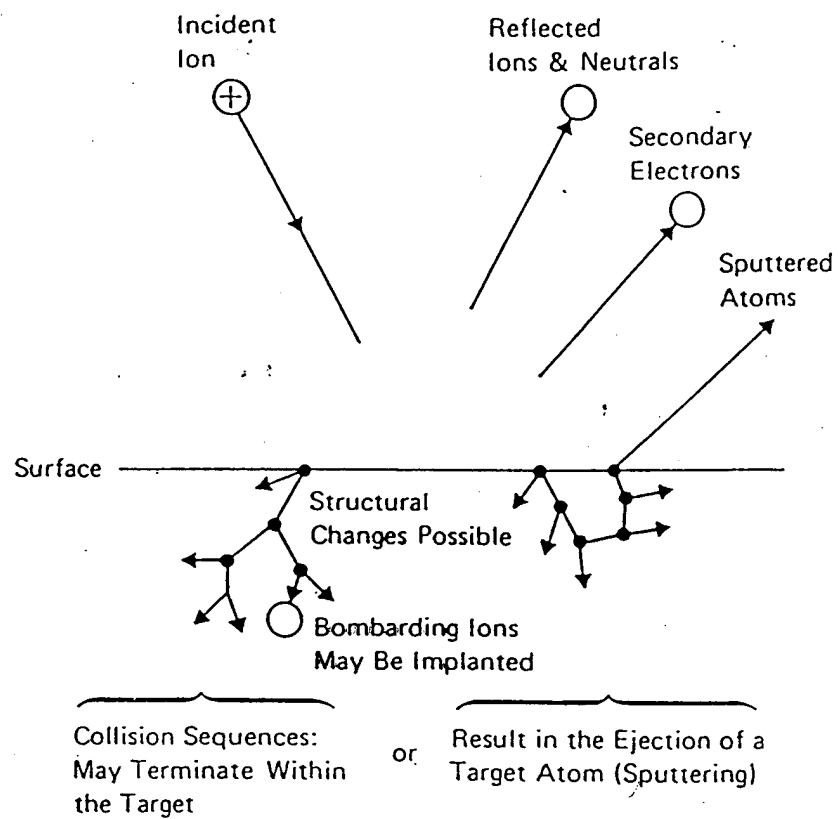
Figure 3.2 The sputtering Process.[11]

BELL JAR

Ar (96%)
H (4%)

SUBSTRATE

DC MAGNETRON
SPUTTERHEAD

MDX-1K
POWER SUPPLY
(0-1000 WATTS)

BASE PLATE

COLD CATHODE
GAUGE

THERMOCOUPLE
GAUGE (TC2)

WATER IN
WATER OUT

COLD TRAP

LIQUID
NITROGEN

HIGH
VACUUM
VALVE

CHAMBER VENT

THERMOCOUPLE
GAUGE (TC1)

ROUGHING VALVE

FAN

FORELINE
VALVE

MECHANICAL
VACUUM
PUMP

DIFFUSION
PUMP
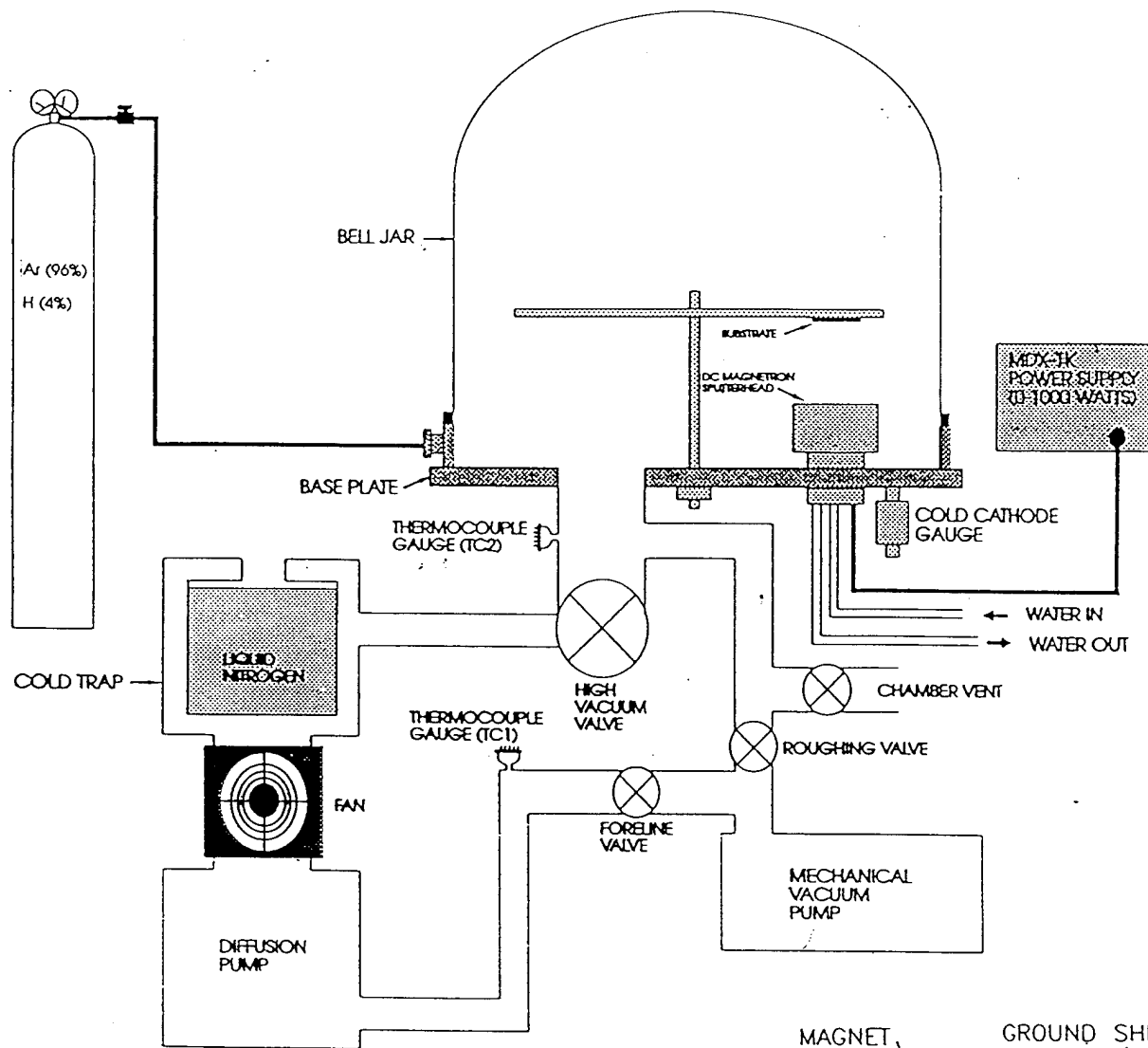
DC magnetron sputtering system at SWTSU.

MAGNET   GROUND SHIELD

WATER COOLING

S

TARGET

N

ELECTRICAL
POWER

S

Cross sectional view of a planar magnetron sputter source
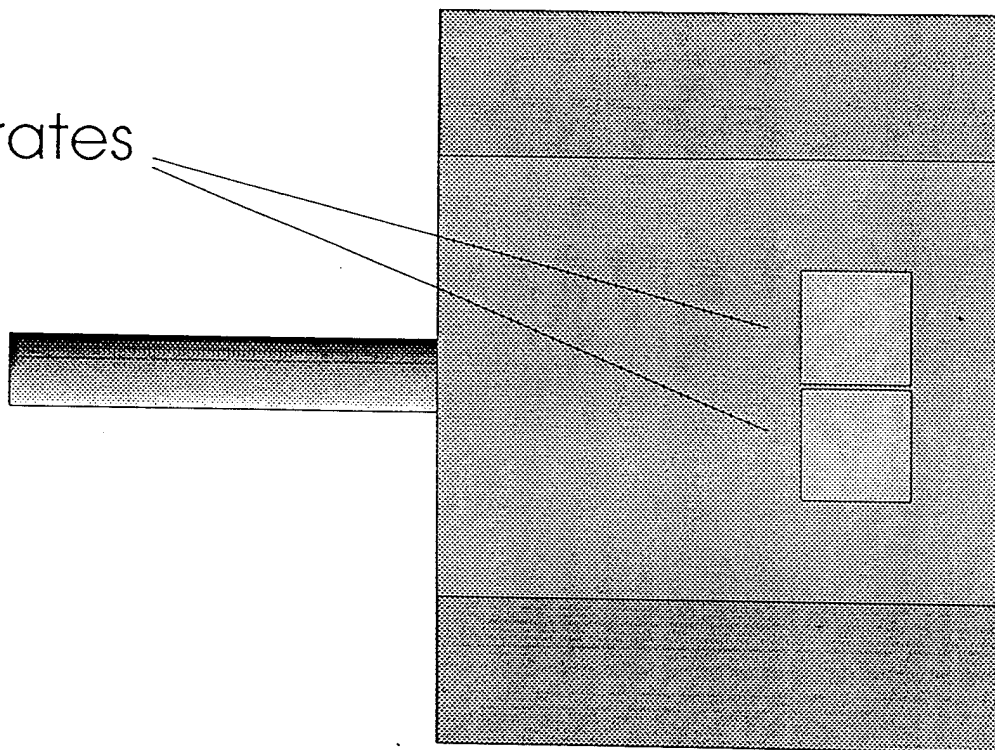
TOP VIEW

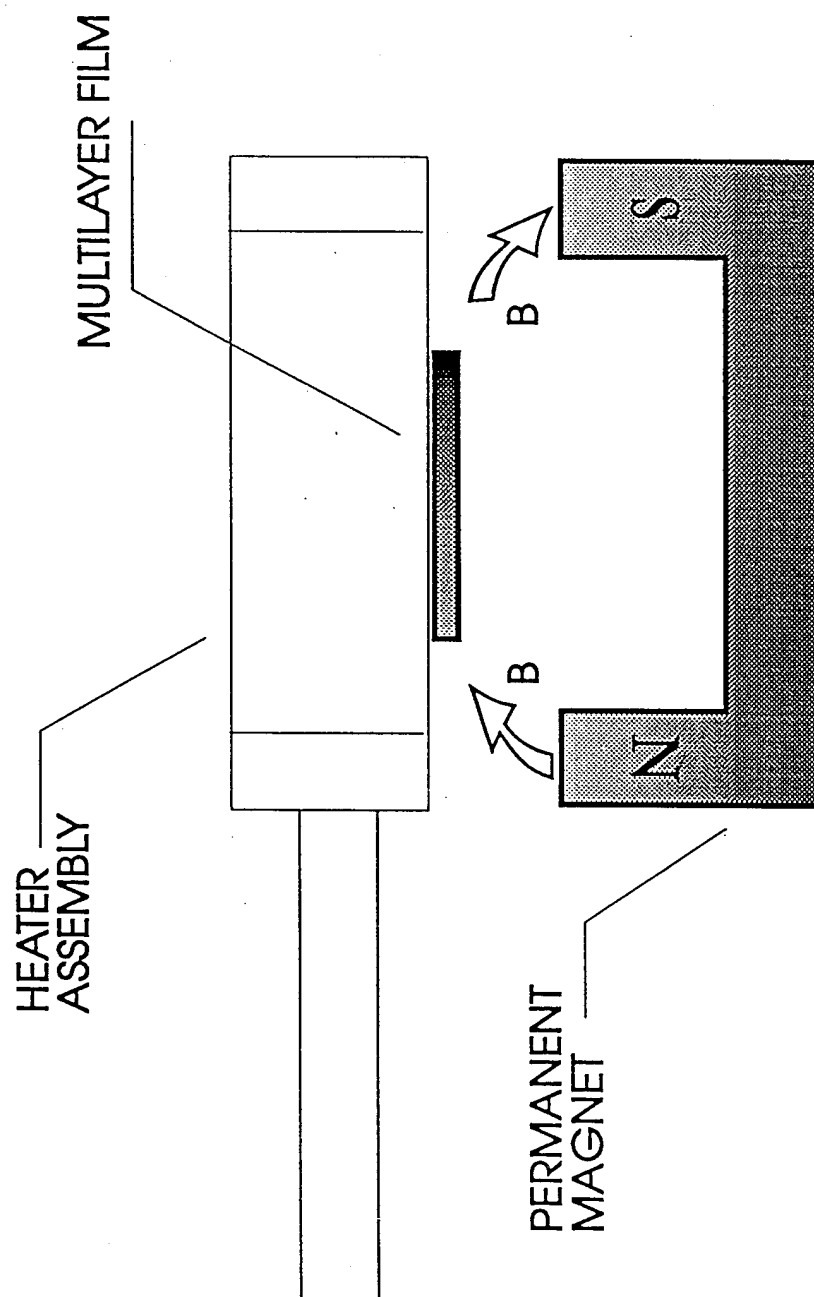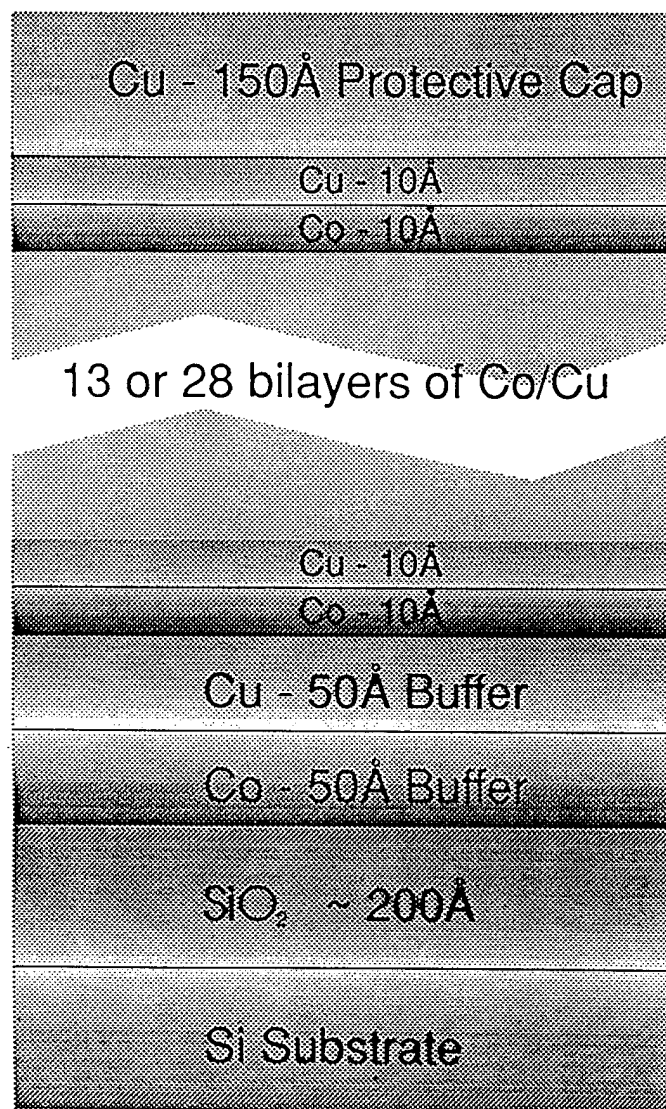Power
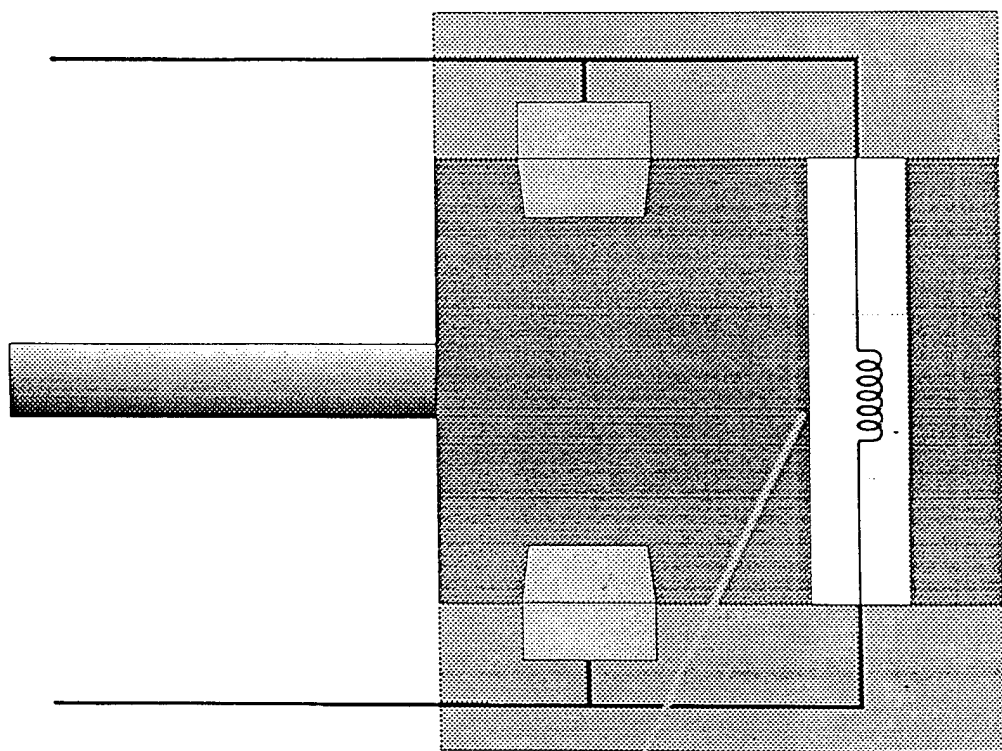
Power

Halogen Lamp

BOTTOM VIEW

Substrates

81

Figure 4.4 A magnetic anisotropy is induced in the plane of a multilayer thin film of Co/Cu by annealing in the magnetic field, B, of a permanent magnet.
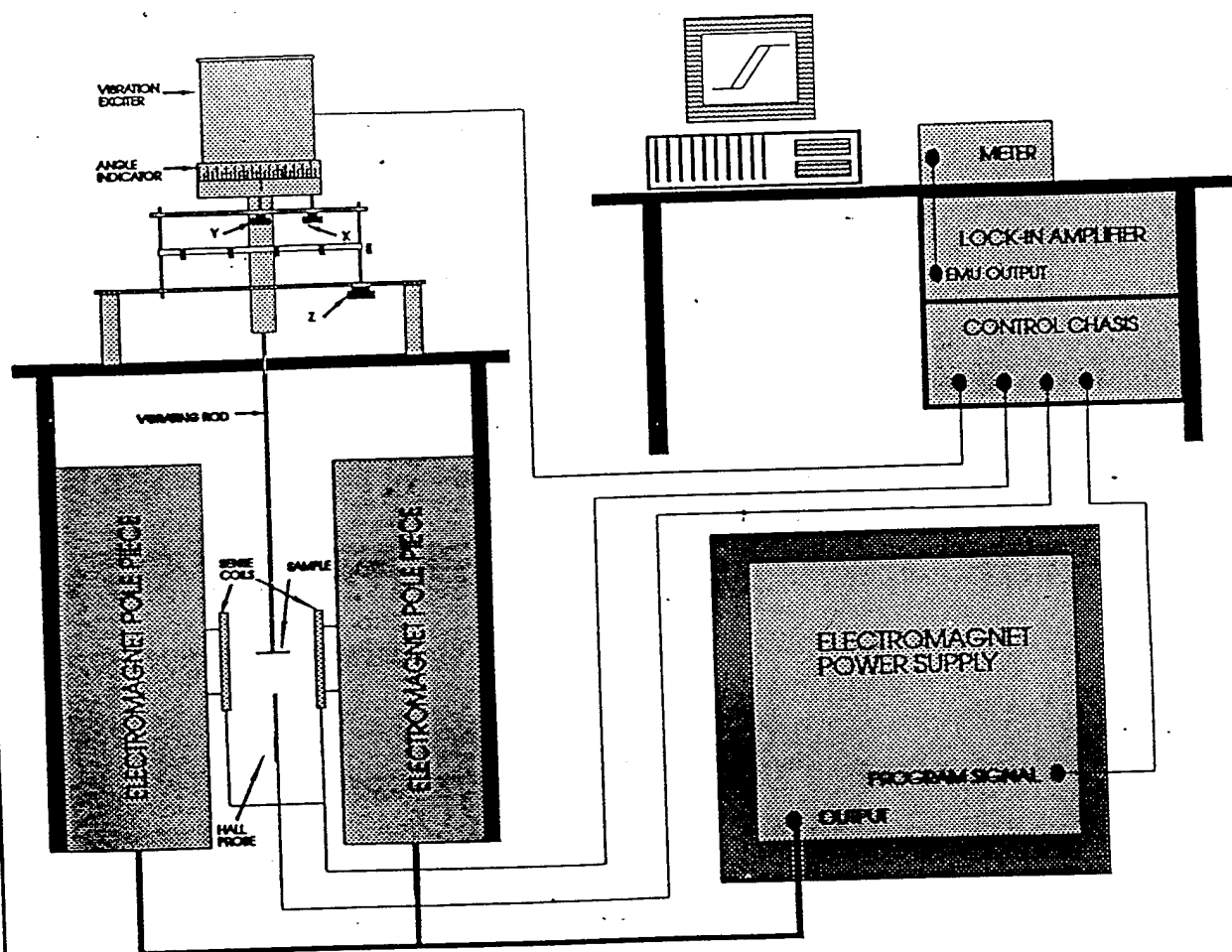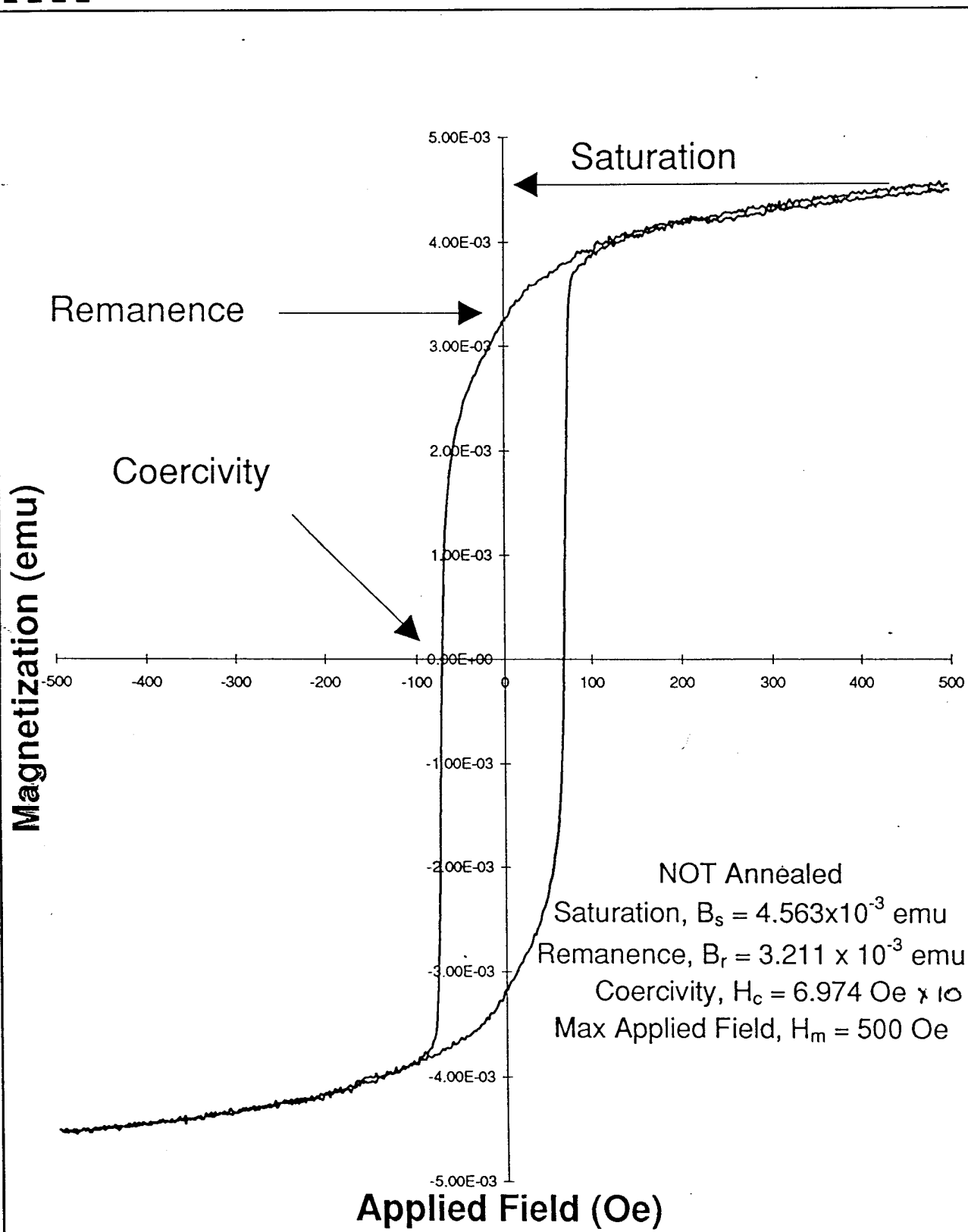
Cu - 150Å Protective Cap

Cu - 10Å

Co - 10Å

13 or 28 bilayers of Co/Cu

Cu - 10Å

Co - 10Å

Cu - 50Å Buffer

Co - 50Å Buffer

$SiO_2 \sim 200$Å

Si Substrate

Cross-section of Co/Cu Film

Figure 4.1 Vibrating sample magnetometer at SWTSU.

Saturation

Remanence

Coercivity

Magnetization (emu)

5.00E-03

4.00E-03

3.00E-03

2.00E-03

1.00E-03

0.00E+00

-1.00E-03

-2.00E-03

-3.00E-03

-4.00E-03

-5.00E-03

-500   -400   -300   -200   -100   0   100   200   300   400   500

Applied Field (Oe)

NOT Annealed
Saturation, $B_s = 4.563 \times 10^{-3}$ emu
Remanence, $B_r = 3.211 \times 10^{-3}$ emu
Coercivity, $H_c = 6.974$ Oe x 10
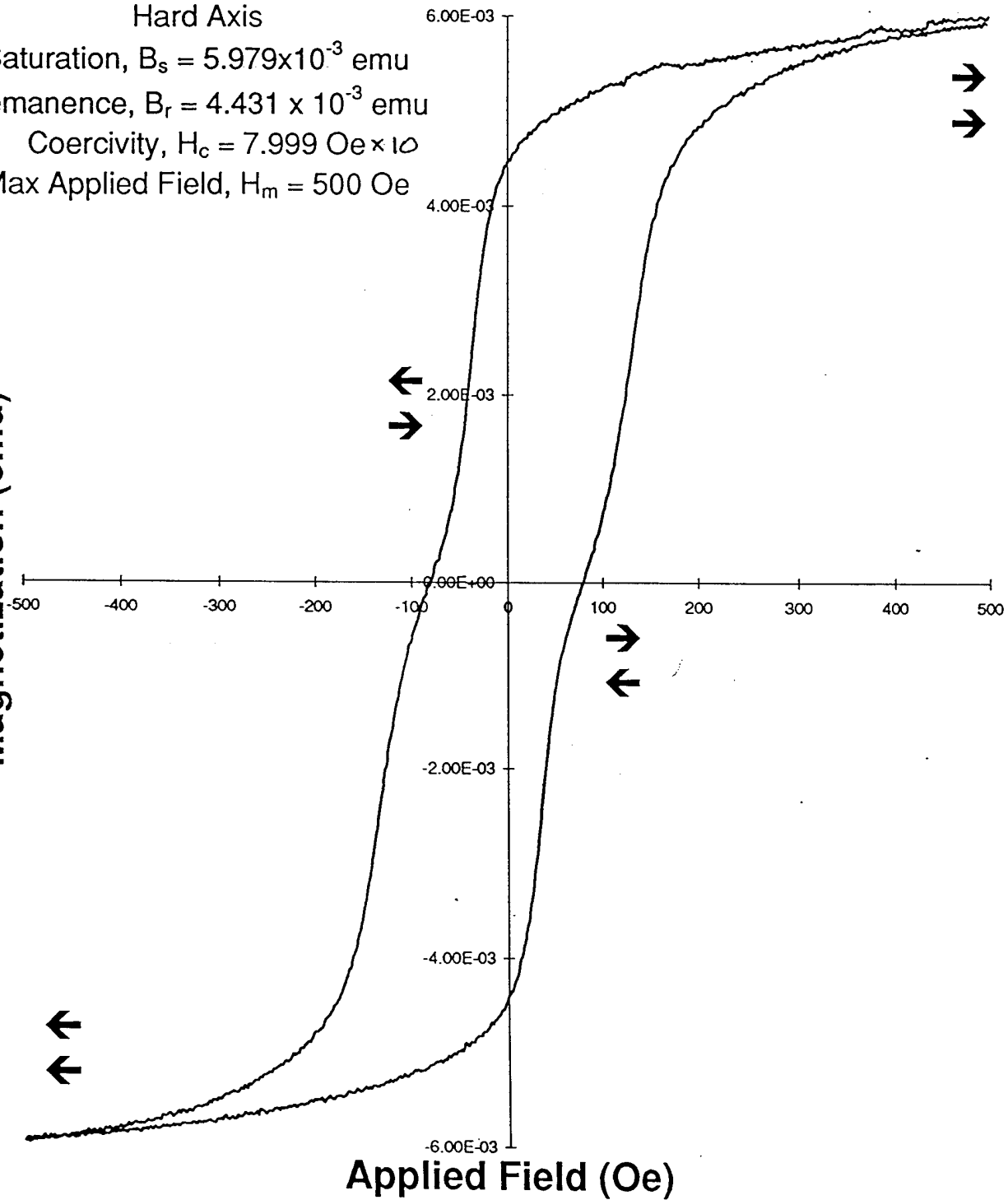Max Applied Field, $H_m = 500$ Oe

Annealed: 450°C
Hard Axis
Saturation, $B_s = 5.979 \times 10^{-3}$ emu
Remanence, $B_r = 4.431 \times 10^{-3}$ emu
Coercivity, $H_c = 7.999$ Oe × 10
Max Applied Field, $H_m = 500$ Oe

Magnetization (emu)

6.00E-03

4.00E-03
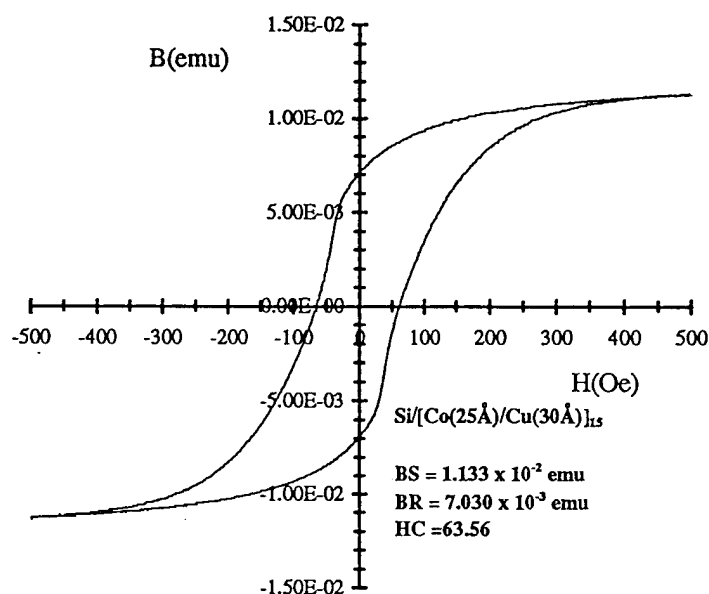
2.00E-03

0.00E+00

-2.00E-03

-4.00E-03

-6.00E-03

-500 -400 -300 -200 -100 0 100 200 300 400 500

Applied Field (Oe)

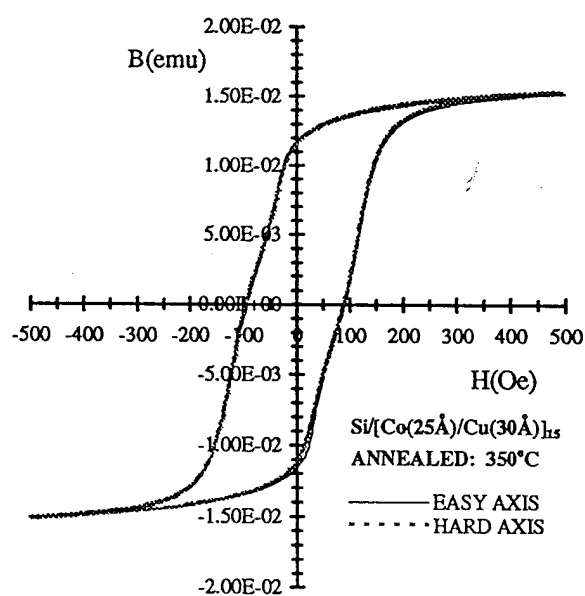Figure 5.15 Hysteresis response of $[Co(25\text{Å})/Cu(30\text{Å})]_{15}$; no anneal.

Figure 5.16 Hysteresis response of $[Co(25\text{Å})/Cu(30\text{Å})]_{15}$; annealed at 350°C; along both the easy axis and·hard axis.
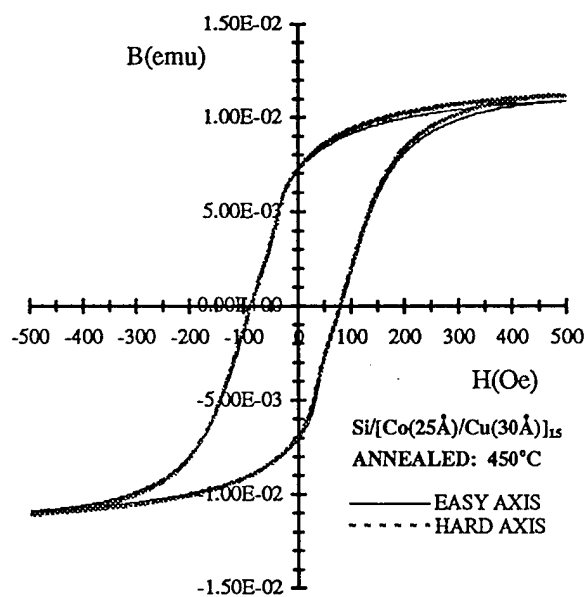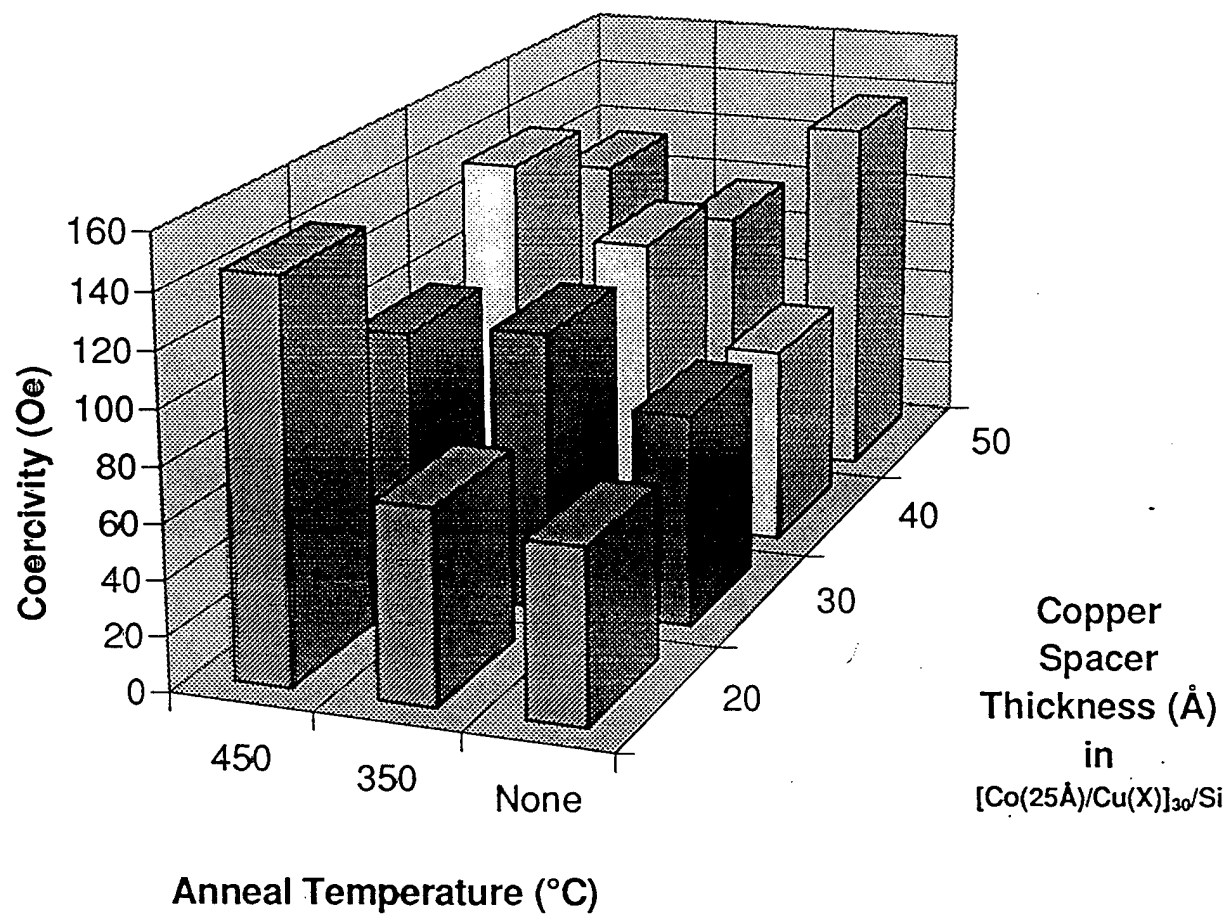
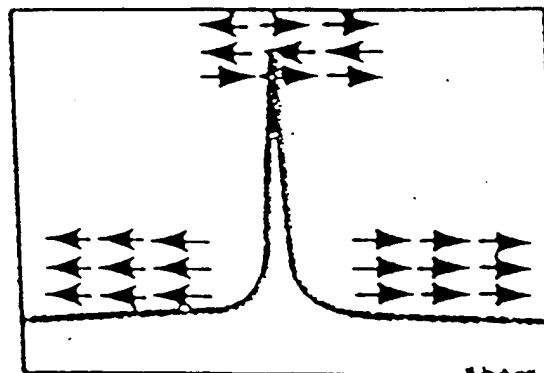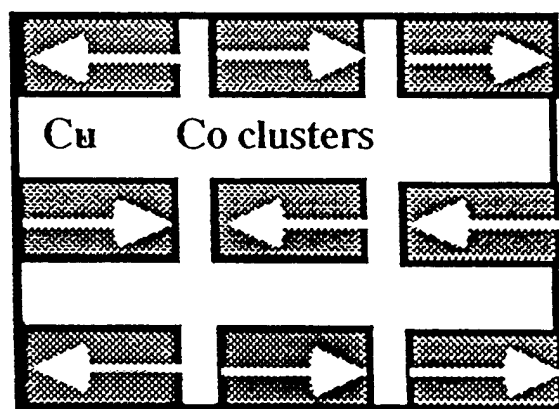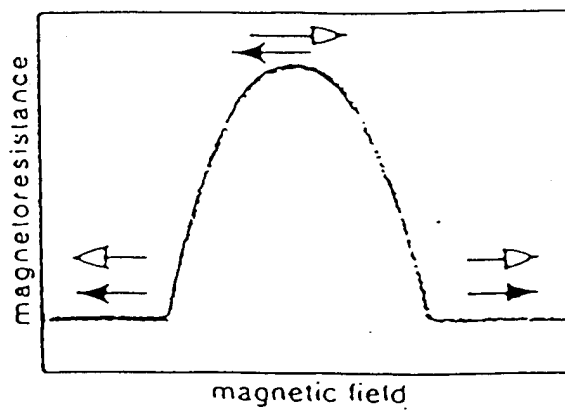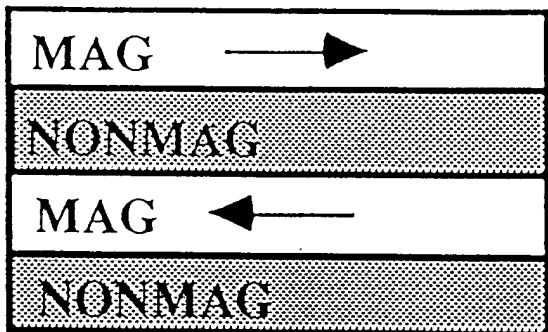Figure 5.17 Hysteresis response of [Co(25Å)/Cu(30Å)]$_{15}$; annealed at 450°C; along both the easy axis and hard axis.

Coercivities in Co/Cu Multilayer Thin Films

Coercivity (Oe)

Copper Spacer Thickness (Å) in [Co(25Å)/Cu(X)]$_{30}$/Si

Anneal Temperature (°C)

MAG ➝

NONMAG

MAG ⬅

NONMAG

magnetoresistance

magnetic field

Cu   Co clusters

ANGLE INDICATOR

METER

MAGNET POLE PIECE

MAGNET POLE PIECE

POGO CONTACTS

SAMPLE

DEWAR
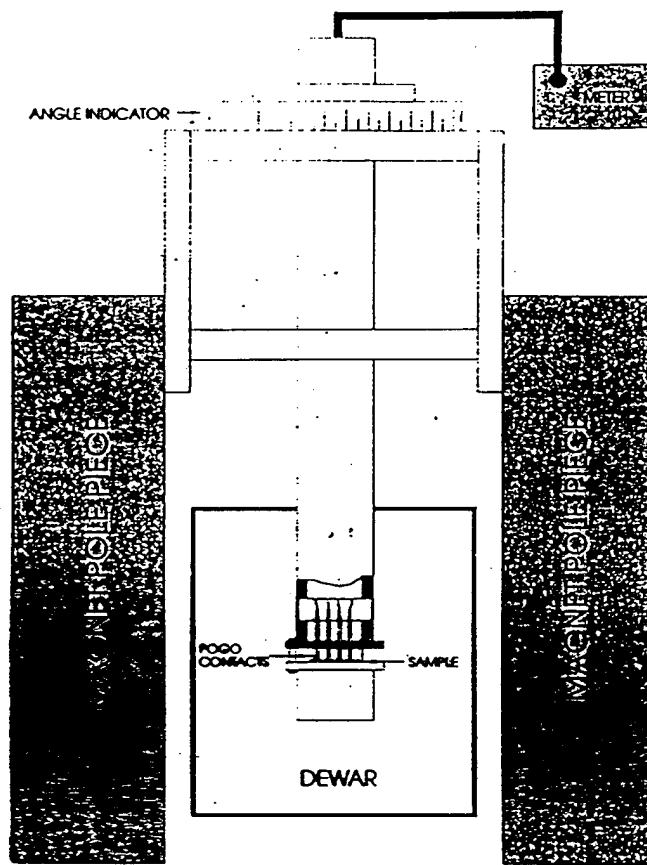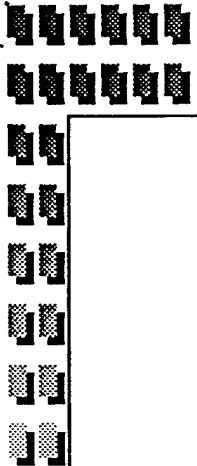
Figure 4.18 The four-point electrical resistance measurement probe at SwRI.

I

V

Co/Cu
MULTILAYER

INDIUM
CONTACTS

Co(25A)/Cu(40A)/Si

GMR = 5.205 %

H_{max} = 120 Oe

FWHM ΔH = 280 Oe
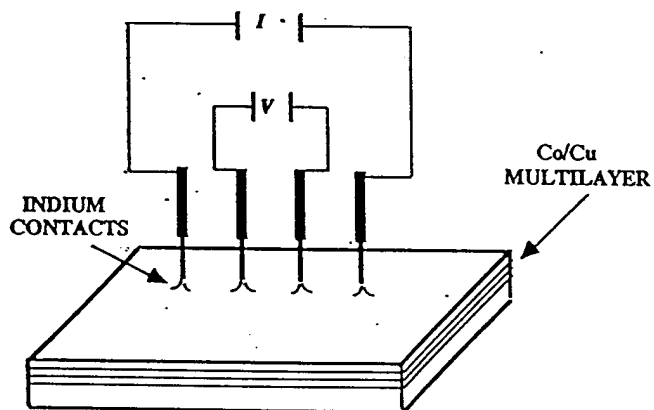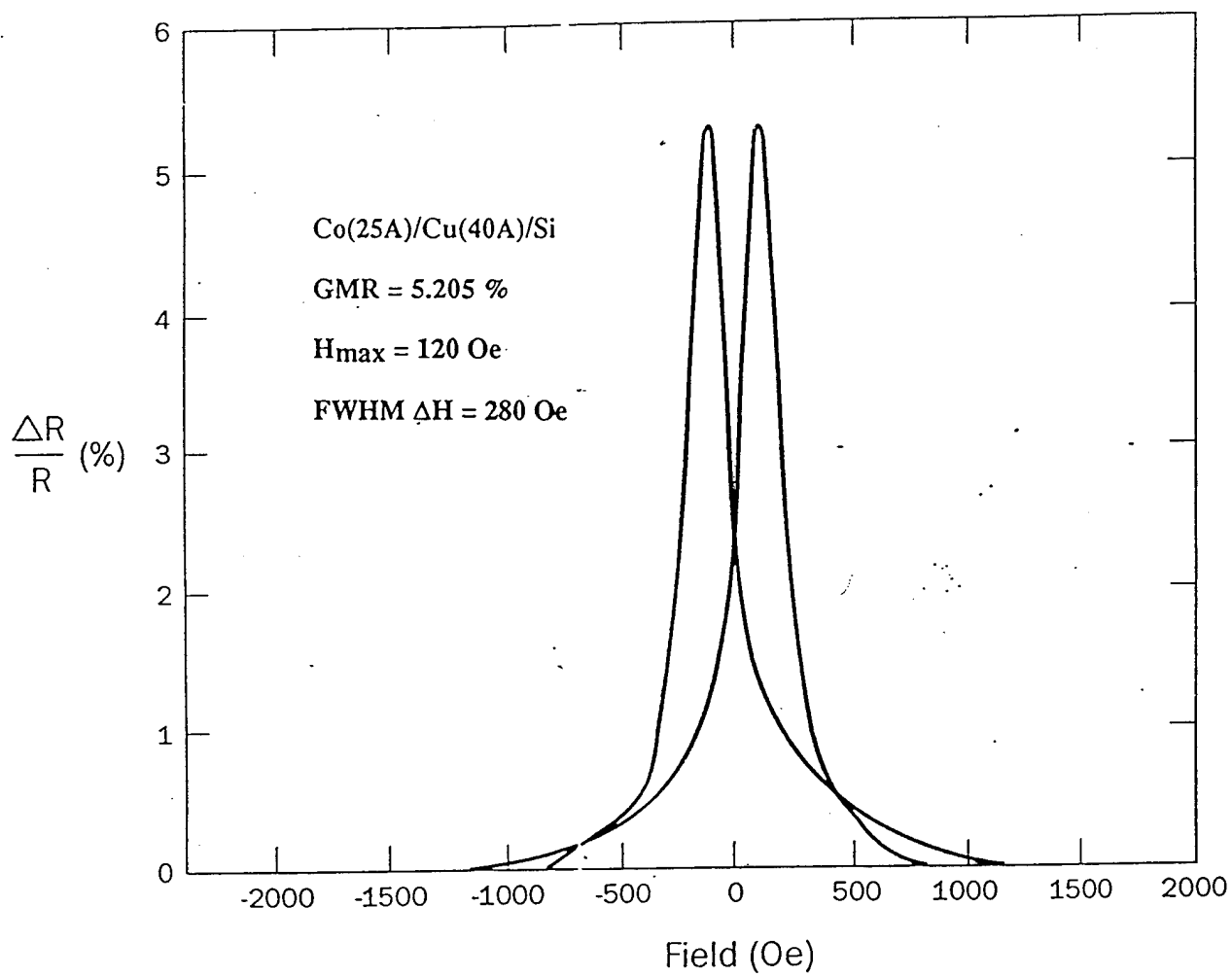
Giant Magnetoresistance (GMR) in Co/Cu Multilayer Thin Films
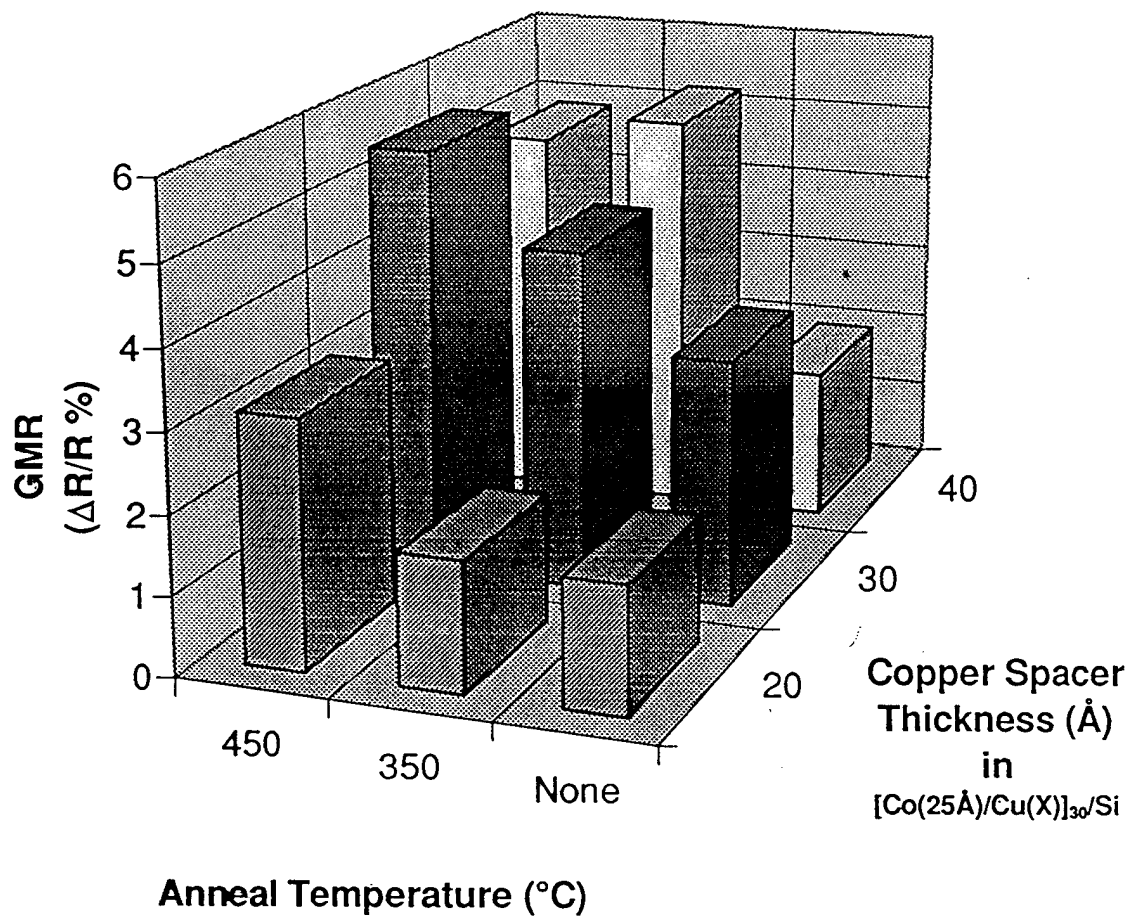
Conclusion and Future Investigation

- Annealing the films increases the coercivity and the GMR

- Discontinuities in the magnetic layers may be responsible for enhanced coercivity and GMR

- X-Ray reflectivity measurements are necessary to determine if discontinuites are present

a)

[Co(5 Å)/Cu(5 Å)]₂₀/Si

[Co(5 Å)/Cu(5 Å)]₂₀/Si	Unannealed (941009A1&B1)	Annealed at 350°C (941010A1&B1)		Annealed at 450°C (941010A2&B2)	
		Easy Axis	Hard Axis	Easy Axis	Hard Axis
B_s (emu)	0.005217	0.004353	0.004284	0.006883	0.006600
B_r (emu)	0.003252	0.003090	0.002983	0.004739	0.004176
B_r/B_s (%)	62.33	70.98	69.63	68.85	63.27
H_c (Oe)	74.48	67.33	68.60	89.73	90.87

b)

[Co(10 Å)/Cu(10 Å)]₁₀/Si

[Co(10 Å)/Cu(10 Å)]₁₀/Si	Unannealed (941007A1&B1)	Annealed at 350°C (941008A&B)		Annealed at 450°C (941009A2&B2)	
		Easy Axis	Hard Axis	Easy Axis	Hard Axis
B_s (emu)	0.009384	0.012260	0.012360	0.008989	0.009057
B_r (emu)	0.006322	0.007887	0.007941	0.006624	0.006423
B_r/B_s (%)	67.37	64.33	64.25	73.70	70.91
H_c (Oe)	50.20	71.28	70.24	161.30	171.00

c)

[Co(25 Å)/Cu(20 Å)]₁₁/Si

[Co(25 Å)/Cu(20 Å)]₁₁/Si	Unannealed (921011A1&B1)	Annealed at 350°C (940921A&B)		Annealed at 450°C (94100J A&B)	
		Easy Axis	Hard Axis	Easy Axis	Hard Axis
B_s (emu)	0.013040	0.015880	0.015880	0.011680	0.011970
B_r (emu)	0.007283	0.011200	0.010600	0.008329	0.008635
B_r/B_s (%)	55.85	70.50	66.75	71.30	72.14
H_c (Oe)	62.90	70.17	71.27	144.60	144.30
$\Delta R/R$ (%)	1.60	1.65		3.13	

Table 5.1 a), b), and c) A summary of the magnetic properties and magnetoresistance of Co/Cu thin films.

a)

[Co(25Å)/Cu(30Å)]₁₅/Si	Unannealed (940927A&B)	Annealed at 350°C (940923A&B)		Annealed at 450°C (941002A&B)	
		Easy Axis	Hard Axis	Easy Axis	Hard Axis
B_s (emu)	0.012360	0.016320	0.016270	0.011770	0.012020
B_r (emu)	0.007136	0.011340	0.010420	0.007136	0.006941
B_r/B_s (%)	57.70	69.50	64.00	60.60	57.70
H_c (Oe)	77.67	102.40	103.10	97.63	96.47
$\Delta R/R_s$ (%)	3.15	4.35		5.48	

b)

[Co(25Å)/Cu(40Å)]₁₅/Si	Unannealed (940928A&B)	Annealed at 350°C (940925A&B)		Annealed at 450°C (941004A&B)	
		Easy Axis	Hard Axis	Easy Axis	Hard Axis
B_s (emu)	0.012260	0.014220	0.014510	0.012850	0.012800
B_r (emu)	0.006444	0.009204	0.008981	0.007426	0.007439
B_r/B_s (%)	52.56	64.70	61.90	57.80	58.12
H_c (Oe)	73.22	110.20	109.30	136.00	136.40
$\Delta R/R_s$ (%)	1.93	5.21		4.85	

c)

[Co(25Å)/Cu(50Å)]₁₅/Si	Unannealed (940926A&B)	Annealed at 350°C (940929A&B)		Annealed at 450°C (941011A2&B2)	
		Easy Axis	Hard Axis	Easy Axis	Hard Axis
B_s (emu)	0.013480	0.012070	0.012210	0.011480	0.011720
B_r (emu)	0.009143	0.007670	0.007694	0.006717	0.006197
B_r/B_s (%)	67.80	63.50	63.00	58.51	52.88
H_c (Oe)	136.20	96.09	96.11	113.20	112.80
$\Delta R/R_s$ (%)		3.9			

Table 5.2 a), b), and c) A summary of the magnetic properties and magnetoresistance of Co/Cu thin films.

Table 5.3 Magnetoresistance $\Delta R/R = (R_{MAX}-R_{MIN})/R_{MIN}$ in perecent for Co/Cu.

STRUCTURE	GMR(%)		
	NO ANNEAL	350°C ANNEAL	450°C ANNEAL
[Co(25Å)/Cu(50 Å)]$_{15}$/Si		3.9	
[Co(25Å)/Cu(40Å)]$_{15}$/Si	1.93	5.21	4.85
[Co(25Å)/Cu(30Å)]$_{15}$/Si	3.15	4.35	5.48
[Co(25Å)/Cu(20Å)]$_{15}$/Si	1.60	1.65	3.13

Table 5.4 Half-Width $\Delta H(Oe)$ for peak GMR for Co/Cu.

STRUCTURE	HALF WIDTH(Oe)		
	NO ANNEAL	350°C ANNEAL	450°C ANNEAL
[Co(25Å)/Cu(40Å)]$_{15}$/Si	320	280	350
[Co(25Å)/Cu(30Å)]$_{15}$/Si	300	210	300
[Co(25Å)/Cu(20Å)]$_{15}$/Si	800	310	320

Table 5.5 Field values $H_{MAX}(Oe)$ at peak GMR for Co/Cu.

STRUCTURE	$H_{MAX}(Oe)$ peak GMR		
	NO ANNEAL	350°C ANNEAL	450°C ANNEAL
[Co(25Å)/Cu(40Å)]$_{15}$/Si	70	120	130
[Co(25Å)/Cu(30Å)]$_{15}$/Si	70	110	90
[Co(25Å)/Cu(20Å)]$_{15}$/Si	60	60	140

Magnetic Films

Coercivity Modifications in Soft Permalloy Films Synthesized by Dual Ion
Beam Sputtering, L. Tristan, R. Dail, M. Khater, D. Medrano; C. J. Gutierrez,
Physics Dept., Southwest Texas State University, and Steve Michel,
Commonwealth Scientific Corporation.--- Thin films of permalloy ($Ni_{80}Fe_{20}$) were
synthesized using a prototype dual ion beam sputtering system (Commonwealth
Scientific Corporation) equipped with a special substrate stage permitting the
application of a uniform in-plane magnetic field during film growth (~150 Oe) used
for inducing a uniaxial magnetic anisotropy in the films (typically ~5 Oe). The
permalloy films ranged in thickness from 20 - 50 nm, and were deposited at room
temperature onto Ta-buffered oxidized silicon. The presence of ~100 eV ion-beam
assist beams directly aimed at the substrate during film growth consistently
modified the coercive and remnant characteristics of the films. Typically, the non-
ion beam assist modified NiFe films exhibited a coercivity ~1 Oe, while the ion
beam assist modified films exhibit a slightly larger coercivity (~1.5 Oe). Such
small coercivity modifications may prove useful in the construction of useful
GMR-based multilayer magnetic film devices.

Prefer Standard Session

_____
(signature of APS member)

Carlos J. Gutierrez
Dept. of Physics
Southwest Texas State University
San Marcos, TX 78666
(512) 245-2131, 245-8233 (FAX)
CG08@ACADEMIA.SWT.EDU

COERCIVITY MODIFICATIONS IN SOFT PERMALLOY FILMS SYNTHESIZED BY DUAL ION BEAM SPUTTERING

A PRESENTATION FOR THE 1995 TEXAS SECTION
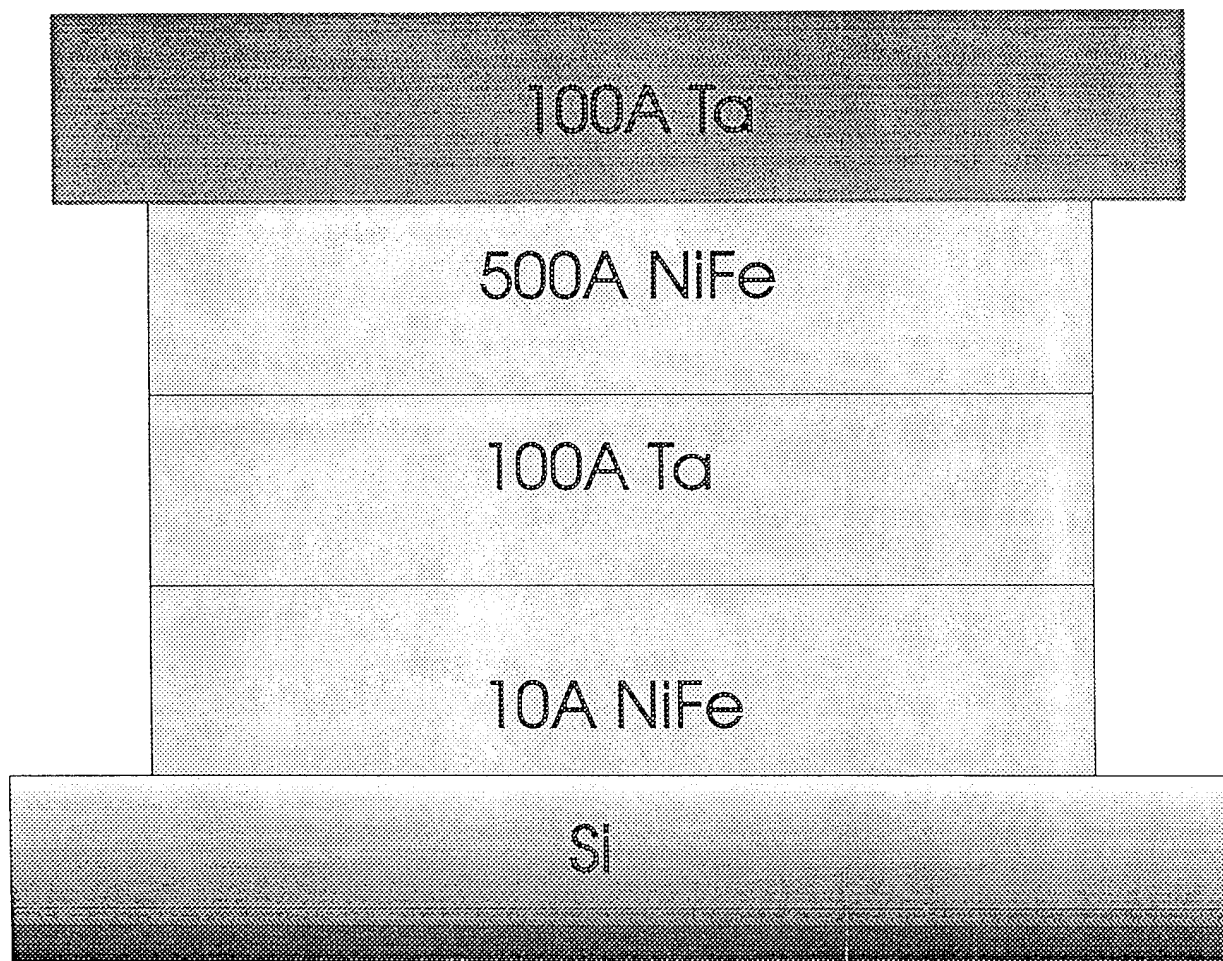MEETING OF THE AMERICAN PHYSICAL SOCIETY

BY
LUIS TRISTAN
GRADUATE STUDENT
DEPT. OF PHYSICS
SOUTHWEST TEXAS STATE UNIVERSITY

AND
*R. DAIL, M. KHATER, D. MEDRANO*
SOUTHWEST TEXAS STATE UNIVERSITY

S. MICHEL
COMMONWEALTH SCIENTIFIC CORP.

*SUPERVISED BY CARLOS GUTIERREZ**
PROFESSOR
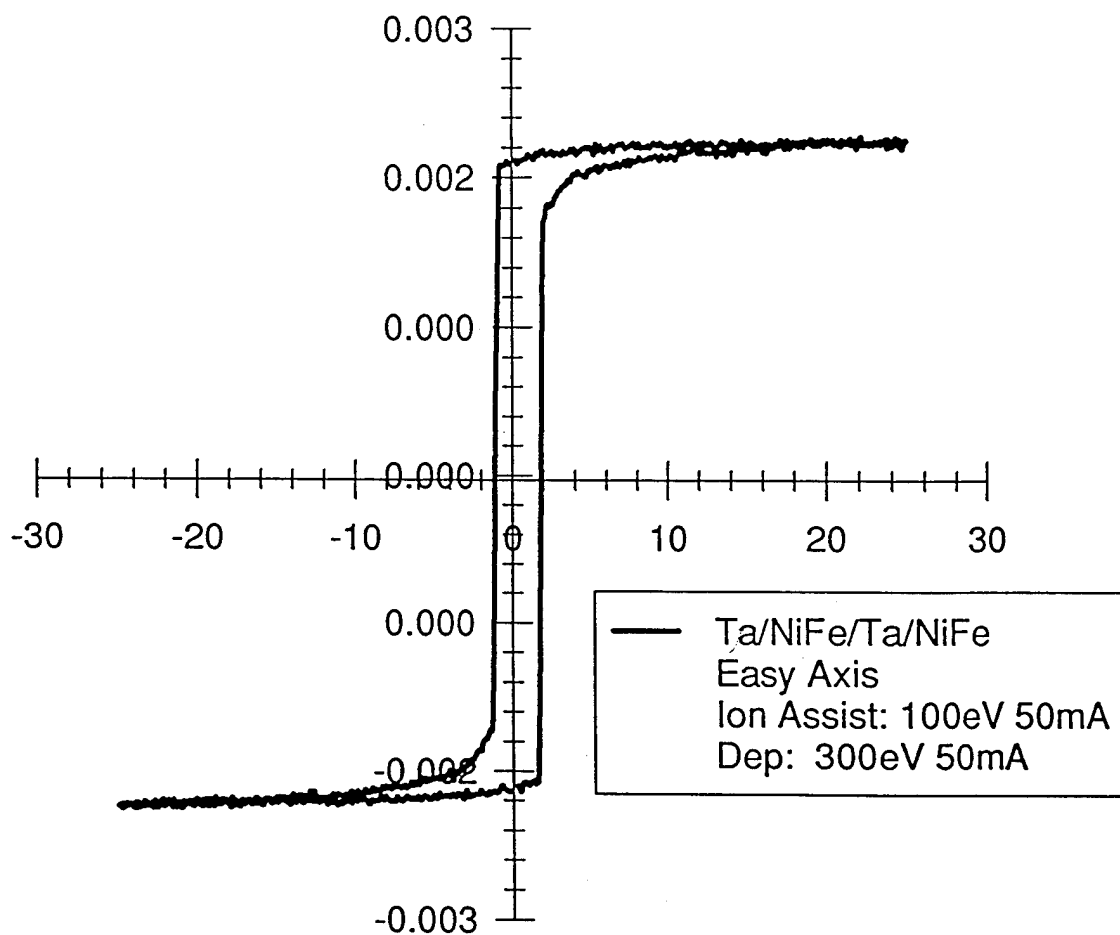*DEPT. OF PHYSICS*
SOUTHWEST TEXAS STATE UNIVERSITY

Typical structure of a NiFe thin film, Ta is used as the
oxidation-protection layer, Ta/NiFe are used as buffer
layers.

SUBSTRATE
STAGE

FILM
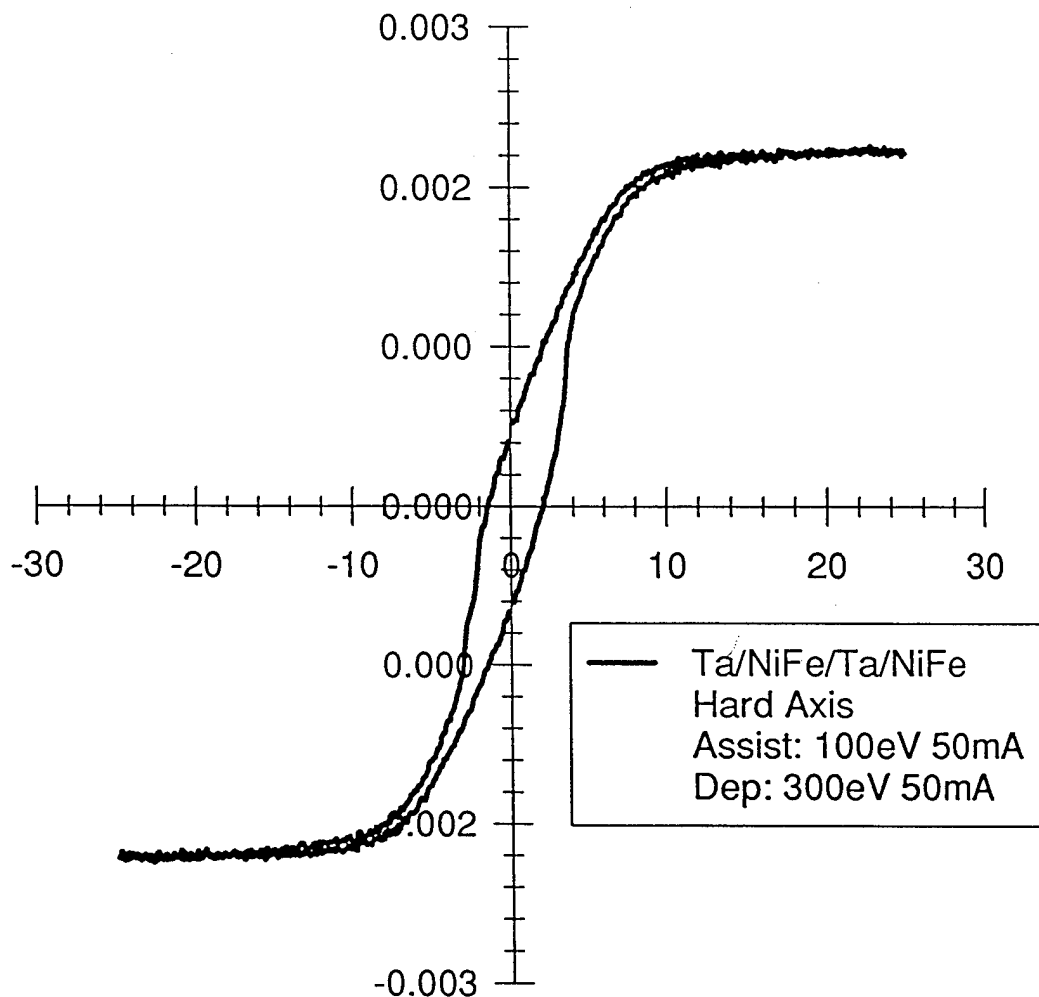
DEPOSITION
BEAM

ASSIST
BEAM

TARGET
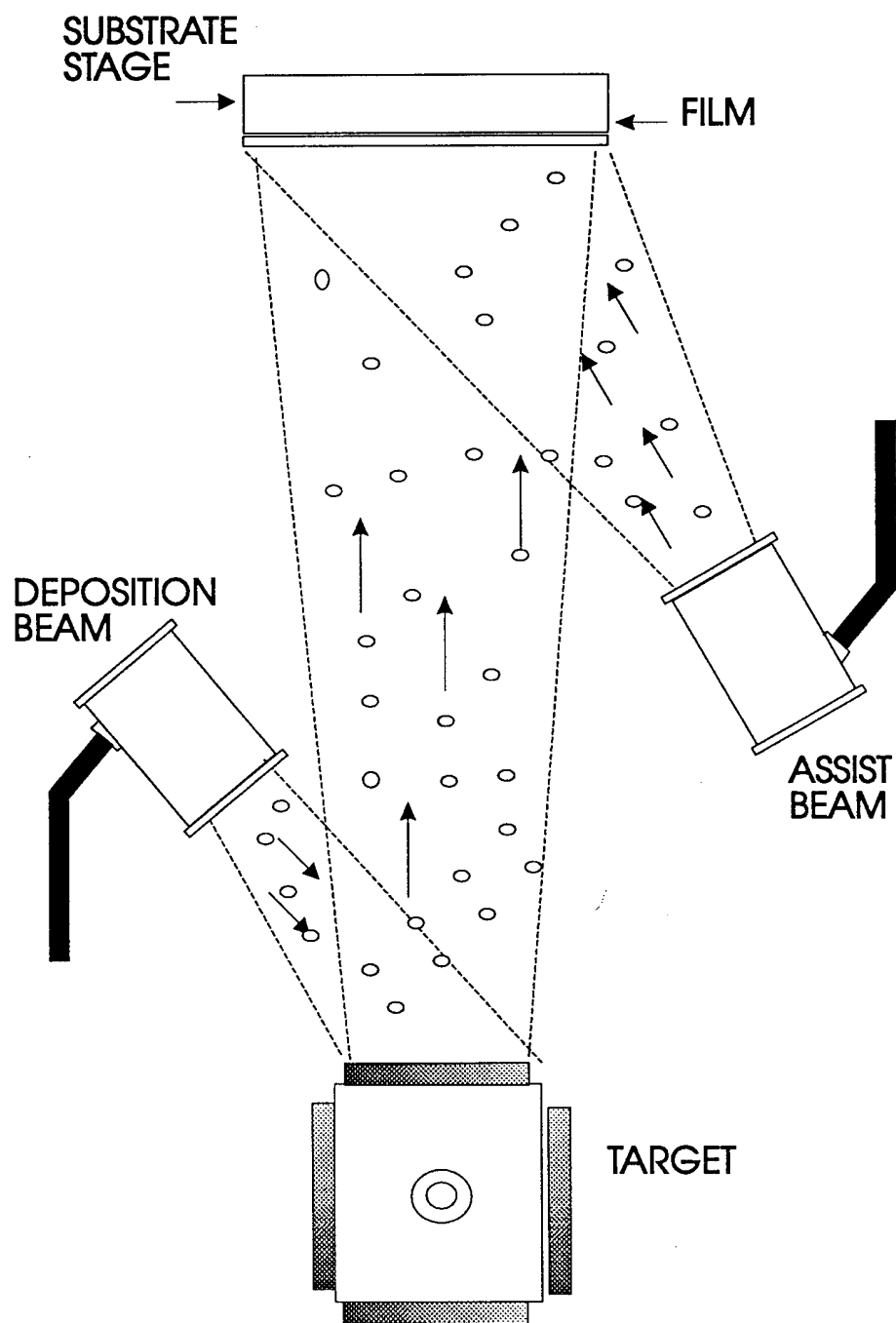
NiFe(10A)/Ta(100A)/NiFe(300A)/Ta(100A)

B-H curve along the easy axis of a 300A NiFe thin film, using slow(300eV, 50mA) deposition

NiFe(10A)/Ta(100A)/NiFe(300A)/Ta(100A)

Legend:
— Ta/NiFe/Ta/NiFe
Hard Axis
Assist: 100eV 50mA
Dep: 300eV 50mA

B-H curve along the hard axis of a 300A NiFe thin film, using slow(300ev, 50mA) deposition beam current.
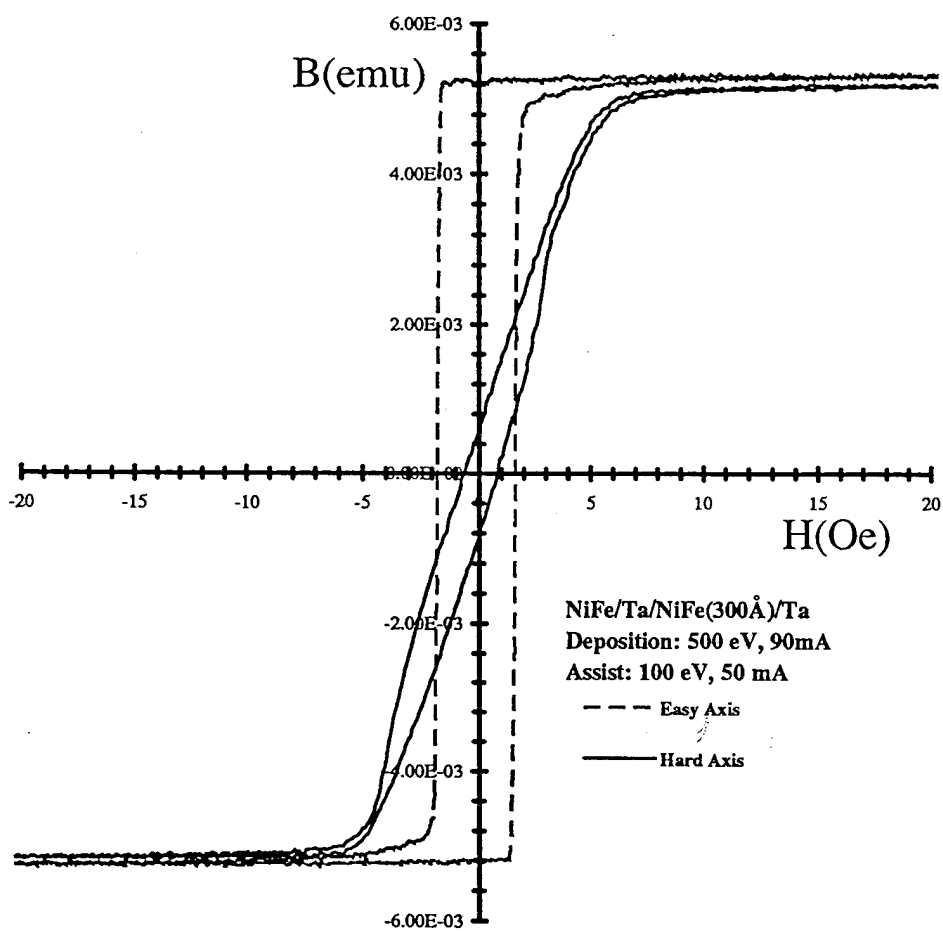
Figure 5.46 Hysteresis response of a permalloy thin film(sample #7) along easy and hard axes.
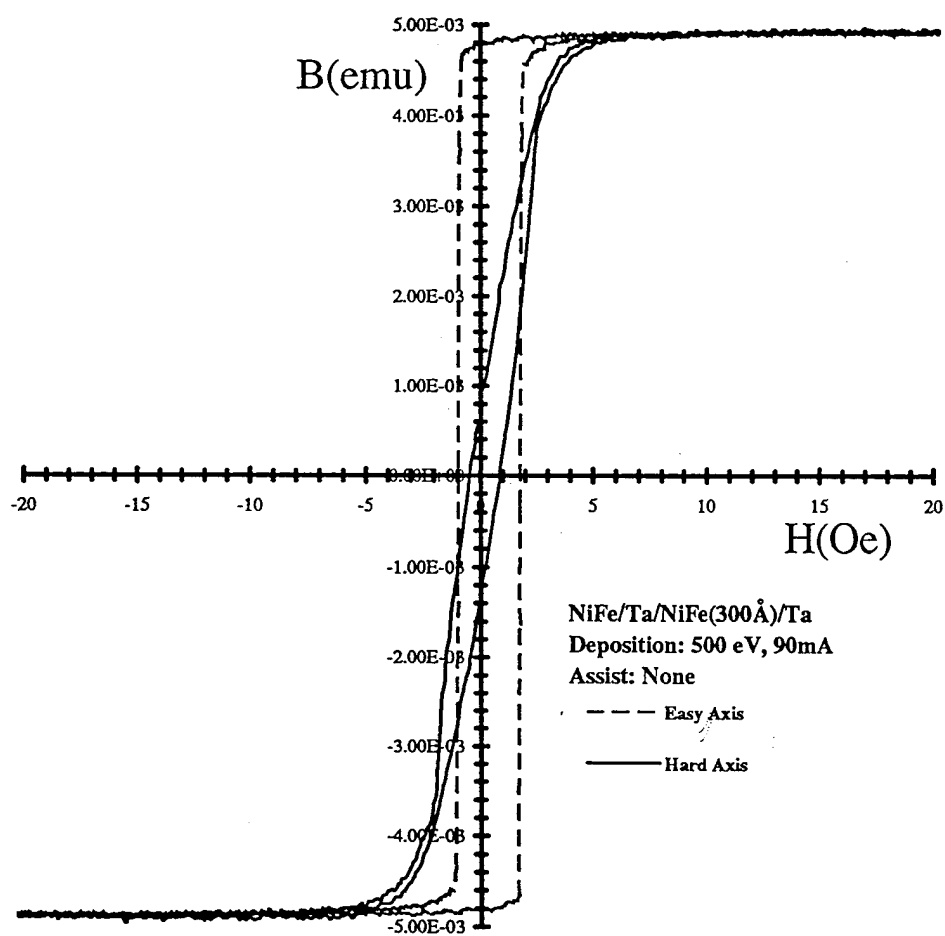
Figure 5.45 Hysteresis response of a permalloy thin film(sample #1) along easy and hard axes.
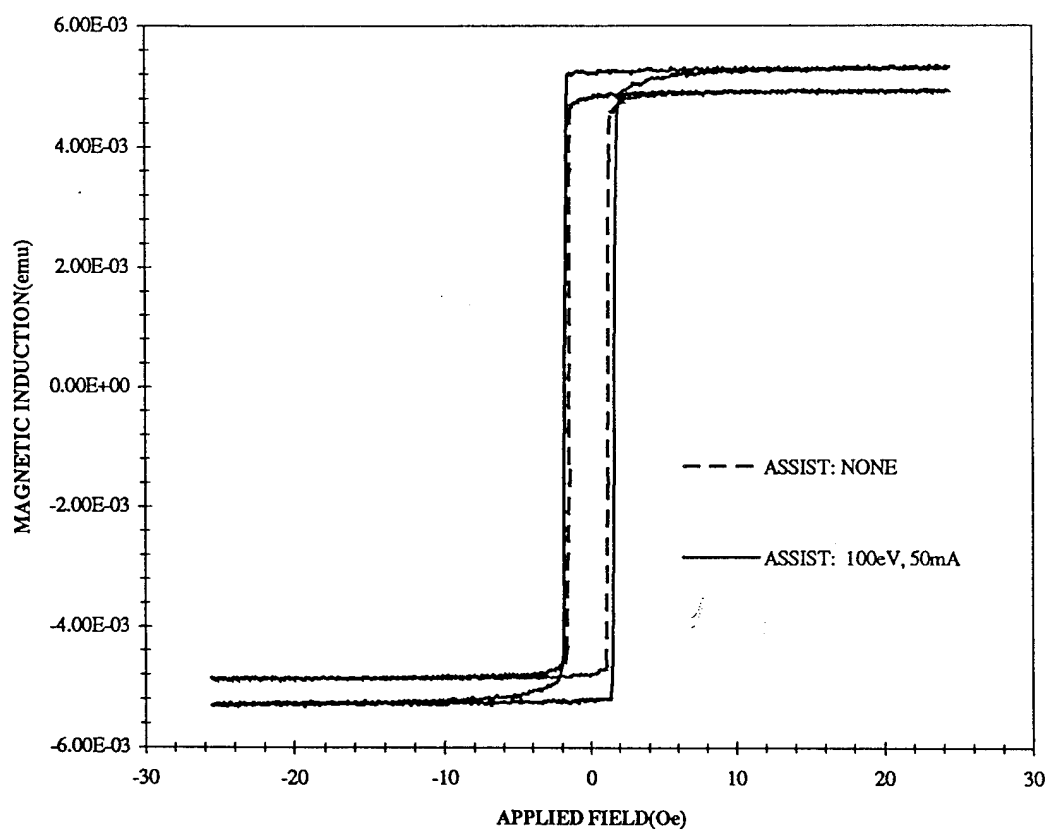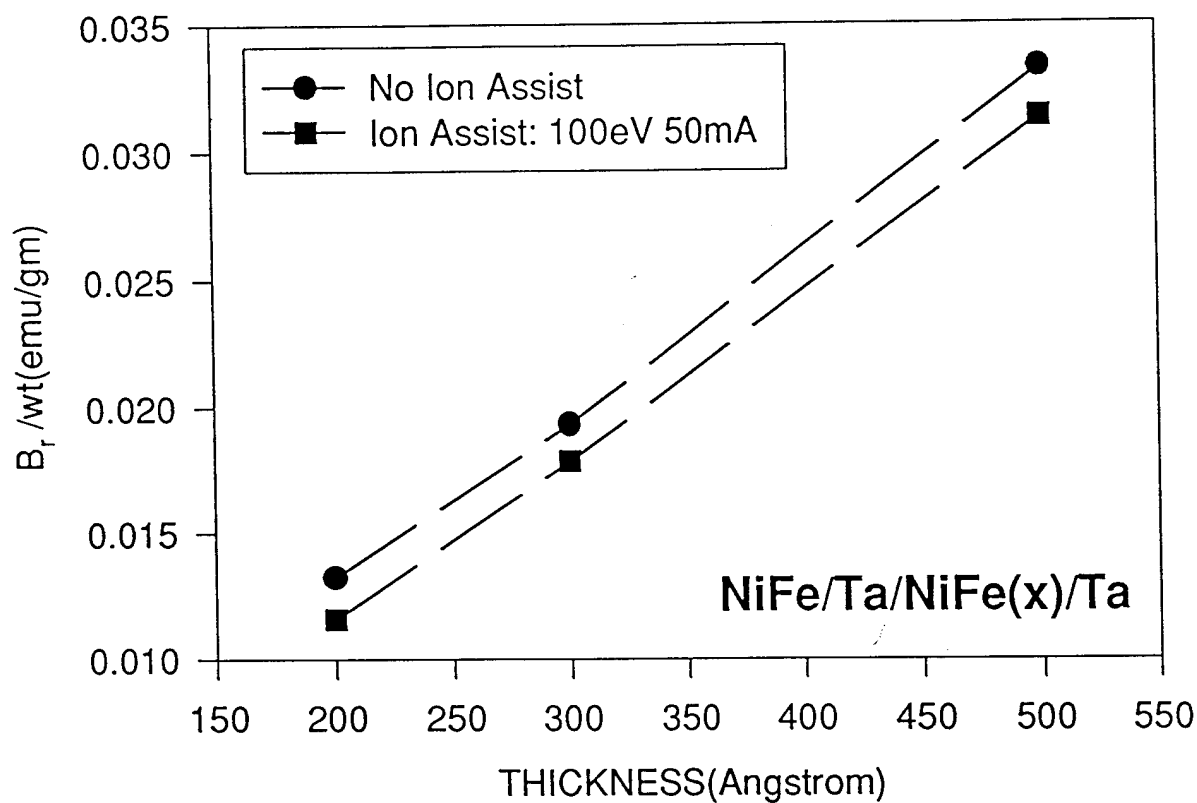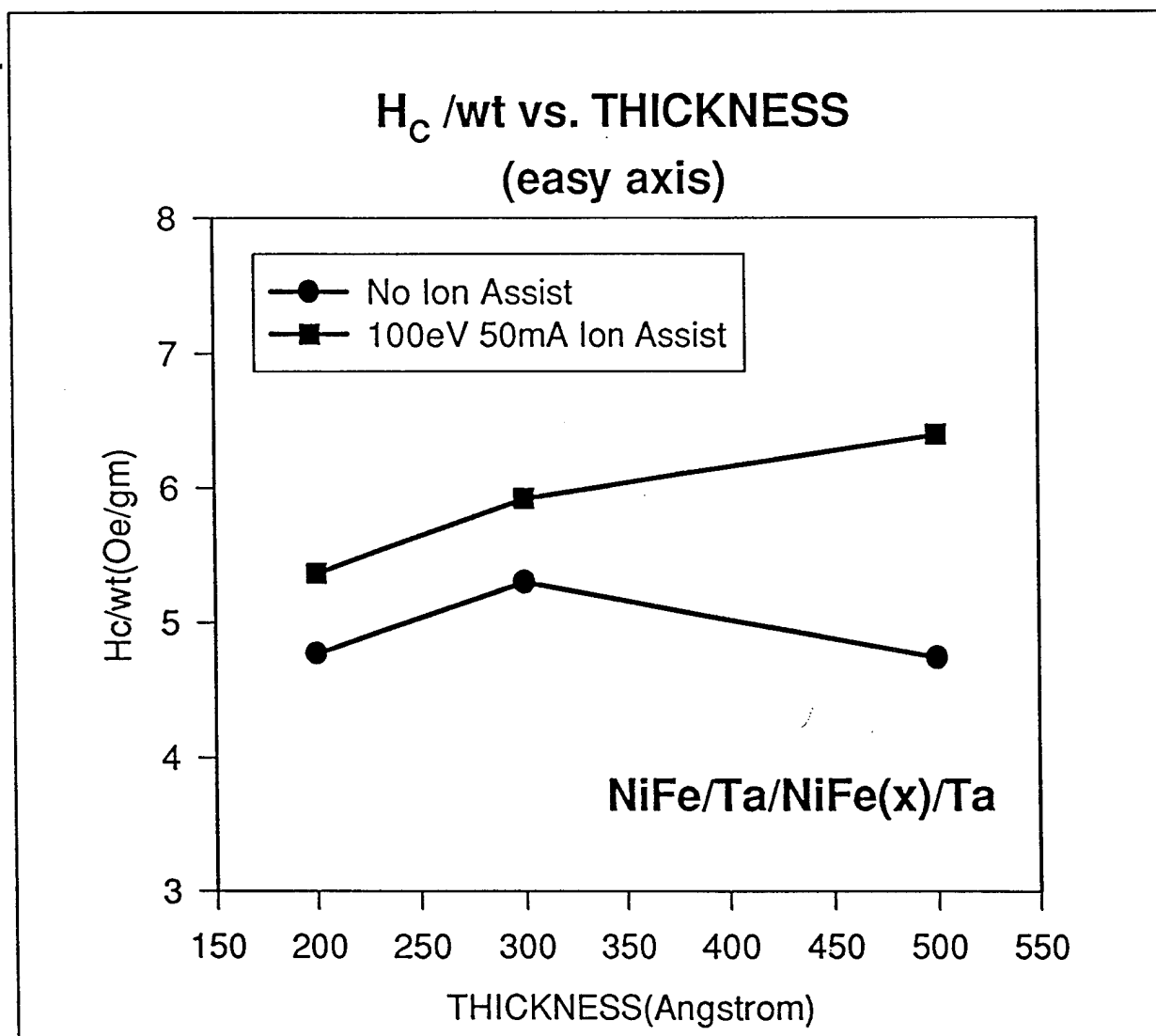
Figure 5.59 Comparison of 100eV, 50mA ion assist and no ion assist for NiFe(200Å). Along the easy axis of magnetization.

REMNANT-SPECIFIC MAGNETIZATION vs THICKNESS
(easy axis)

Ion beam assist lowers the remanence of a thin film, for NiFe/Ta/NiFe(x)/Ta, where x = 200A, 300A, 500A, each point is the average of 6 films.

H$_C$/wt vs. THICKNESS
(easy axis)

- ● No Ion Assist
- ■ 100eV 50mA Ion Assist

NiFe/Ta/NiFe(x)/Ta

Hc/wt(Oe/gm)

THICKNESS(Angstrom)

Ion beam assist modifies the coercivity of a NiFe/Ta/NiFe(x)/Ta, film for thickness x = 200A, 300A, 500A

B_r /wt vs THICKNESS(hard axis)
Ta/NiFe(x)/Ta/NiFe
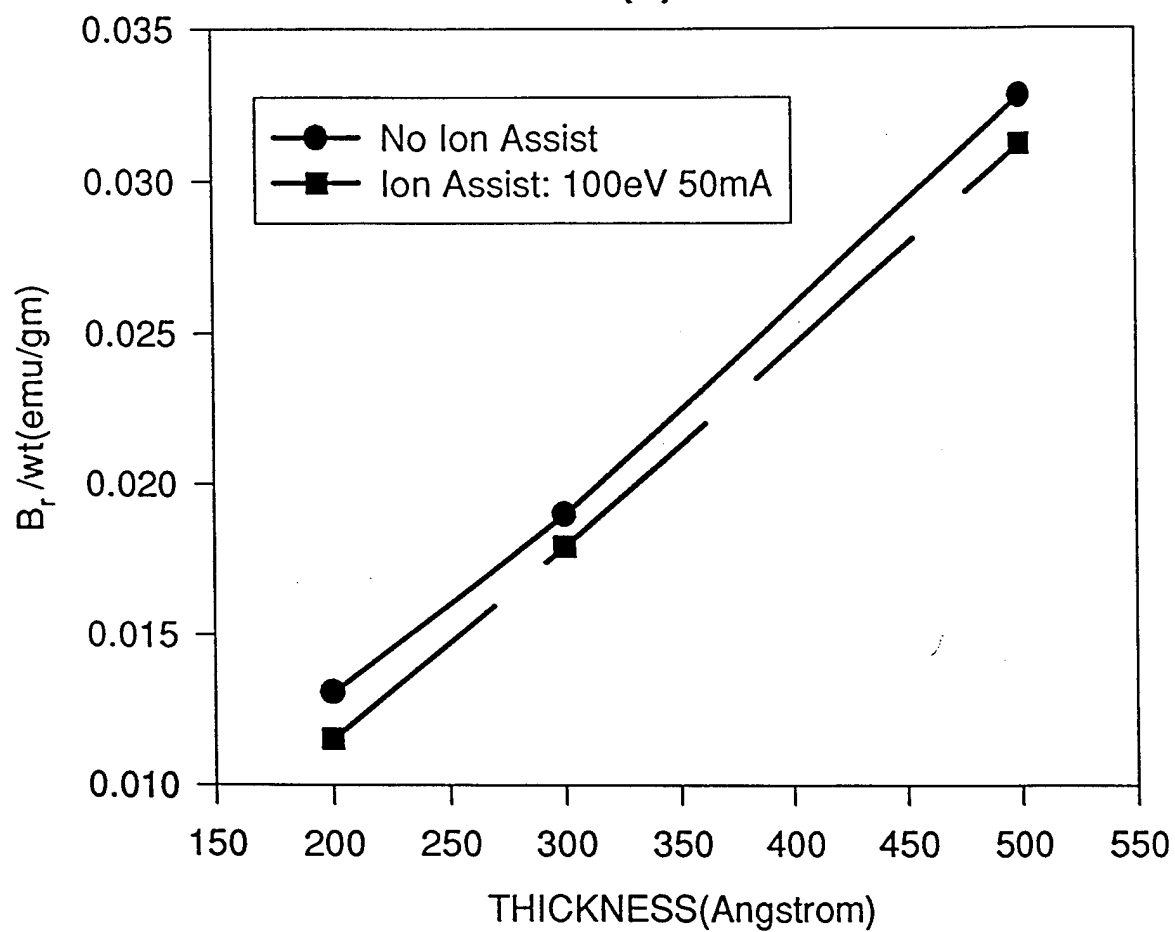
H_c/wt vs THICKNESS (hard axis)
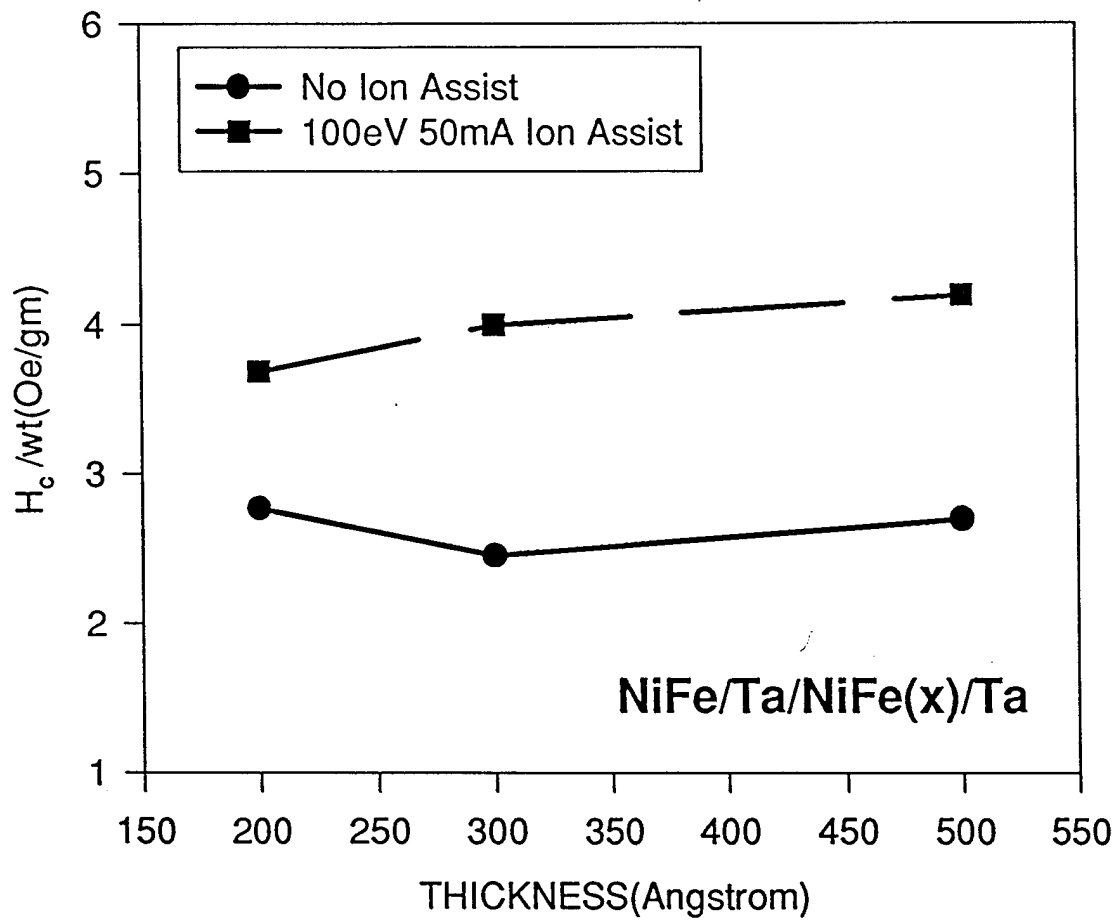
Coercivity modified by ion beam assist for NiFe(x) thickness
x = 200A, 300A, 500A

NiFe(10A)/Ta(100A)/NiFe(300A)/Ta(100A)
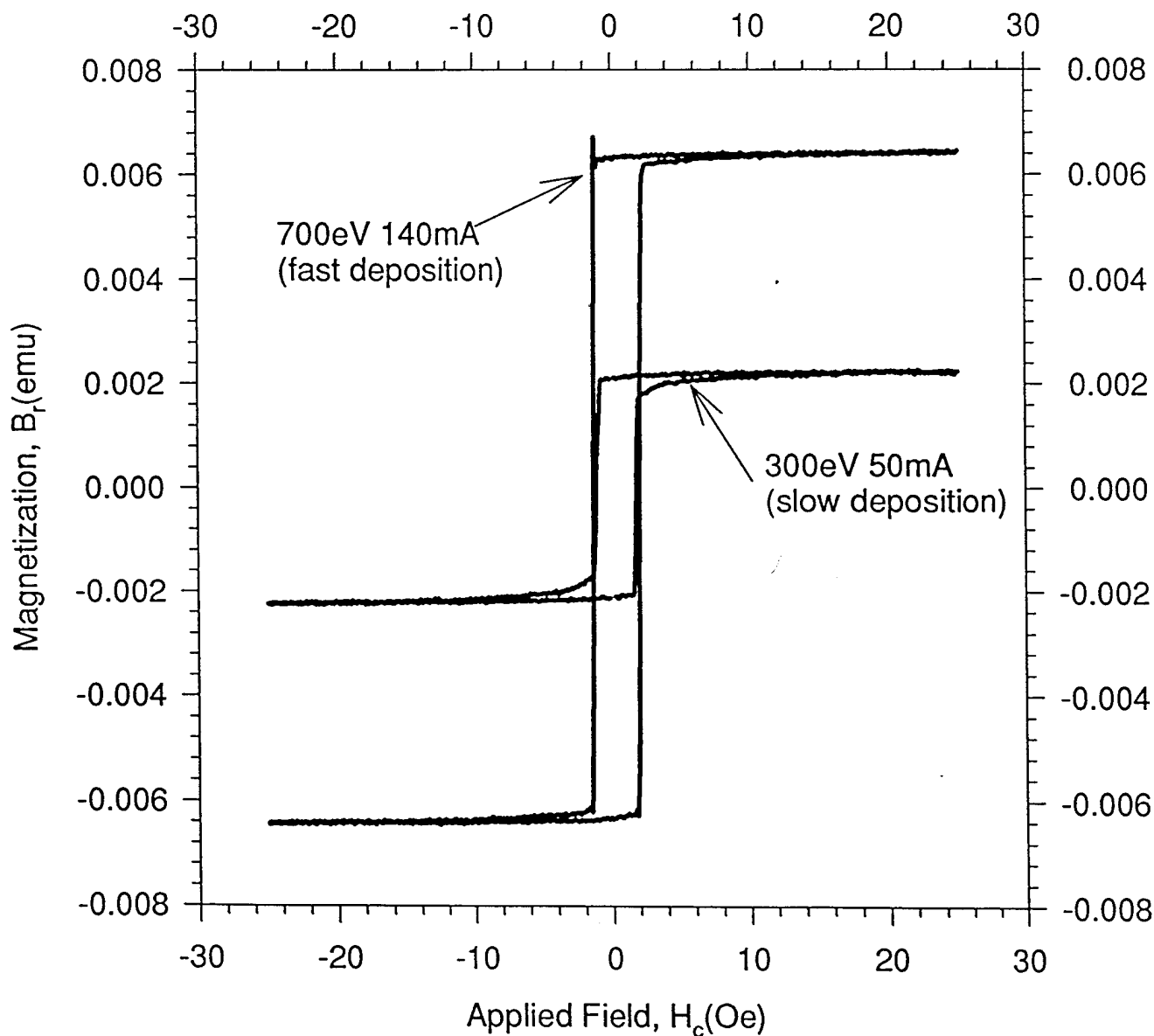
comparison between fast(140mA) beam current deposition,and slow(50mA)
beam current deposition; both films have same thickness

B-H Comparison Along Hard Axis
For Varying Beam Deposition Energy
Ta/NiFe(300A)/Ta/NiFe
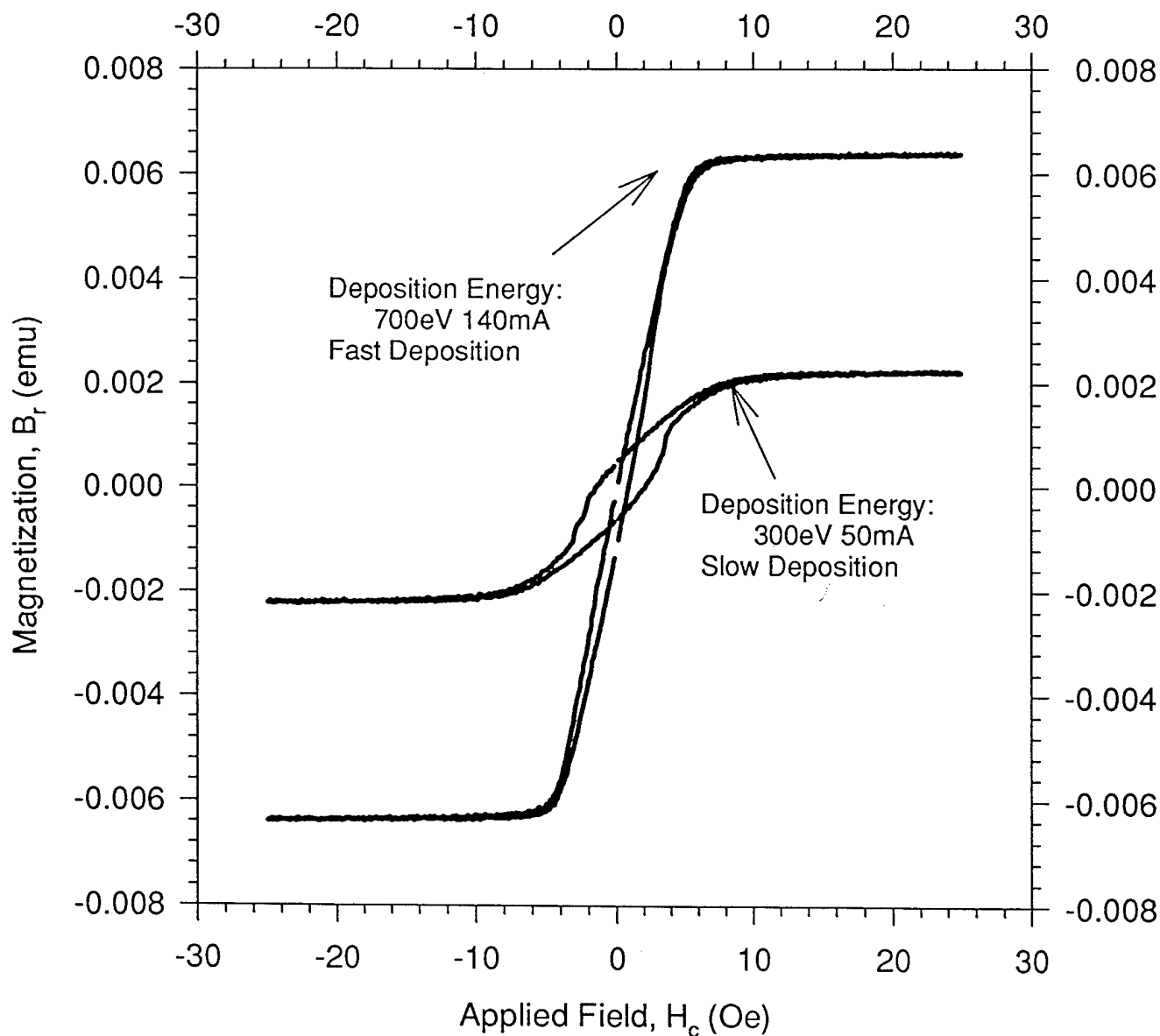
Comparison between slow(300eV, 50mA) beam current deposition and fast(700eV, 140mA) beam current deposition; for films of same thickness

Film Surface Environment Scenarios during Sputtering
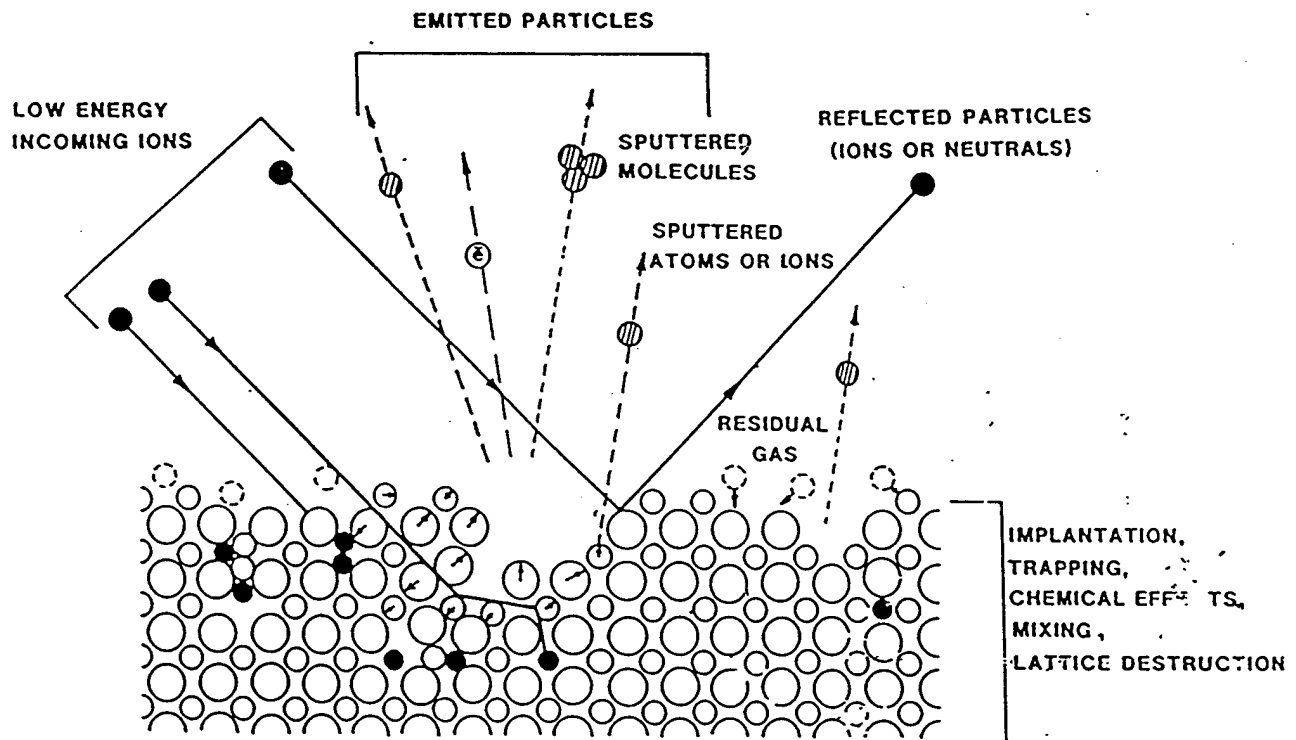
Fig. 2.1. General ion–surface interaction processes.
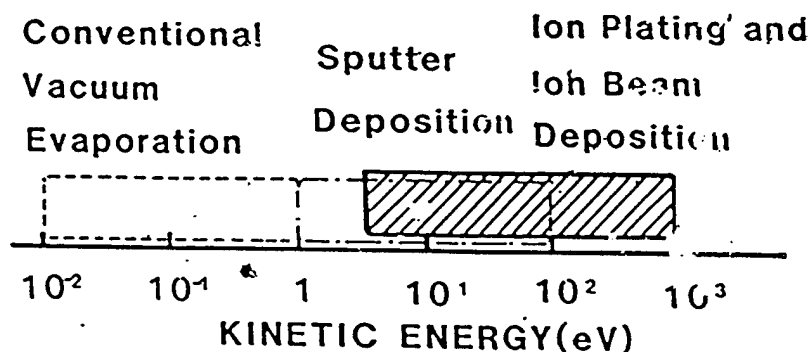
Fig. 4.1. Energy range typical of the preparation methods for film formation. (TAKAGI [1982].)

Ref: P. J. Martin and R. P. Netterfield, Progress in Optics Vol. 23, pp 115–178 (1986)
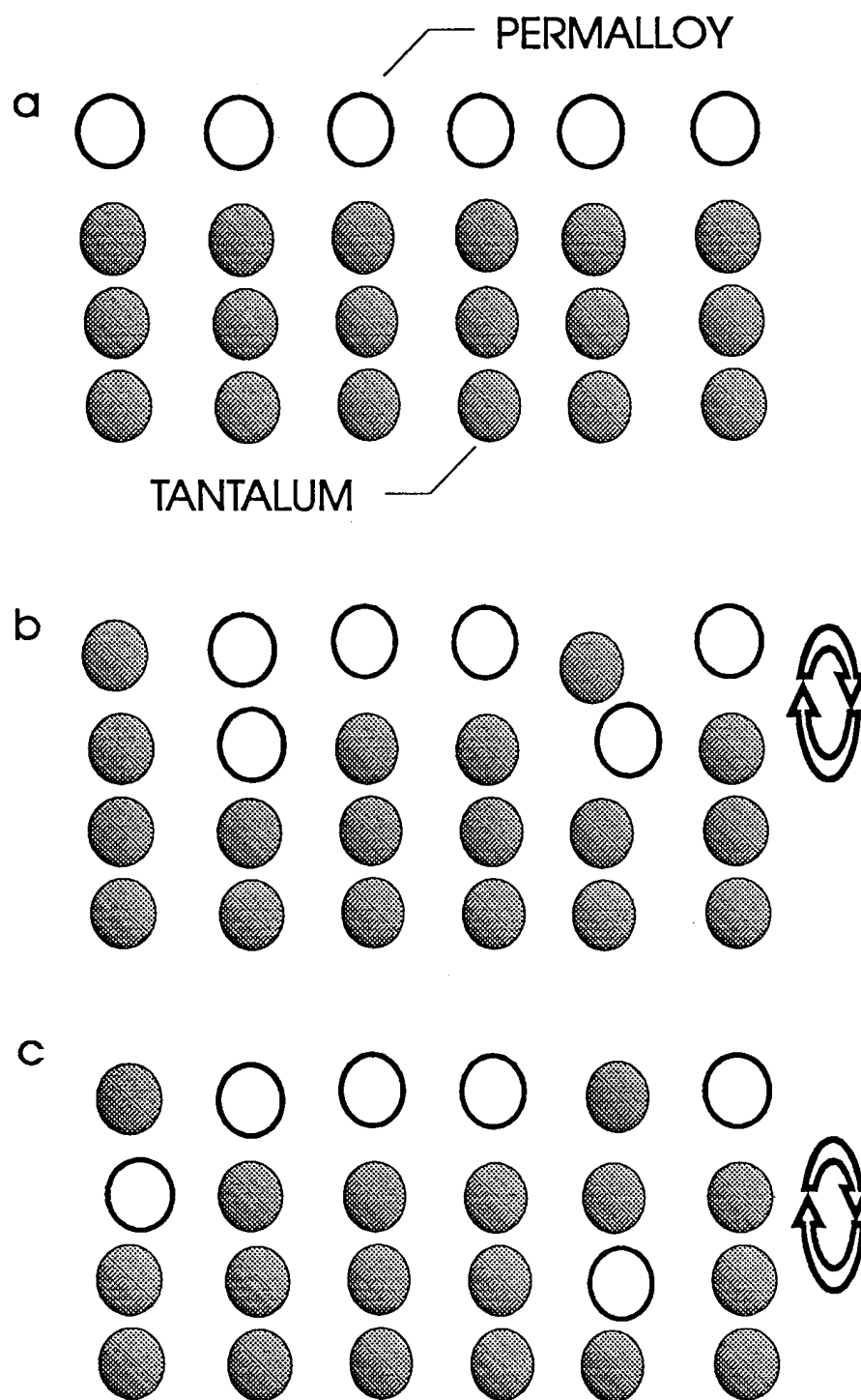
Figure 5.62 Ion beam mixing effect for NiFe ions and Ta: a) no mixing, b), Ta modifies moment of NiFe ion; c) Ta can nullify moment of NiFe.

CONCLUSIONS

1. Increased *Deposition Gun Energy* increases the remanenence, B_r of $Ni_{80}Fe_{20}$ thin films.

2. Presence of *Ion Assist* increases the coercivity, H_c, and decreases the remanence, B_r.

3. From points 1., and 2., above, it is evident that *Ion-Beam Mixing* is responsible for the modification of magnetic properties. Increased deposition energy causes Agitation and mixing between permalloy ions and Ta atoms.

4. These parameters will be exploited for processing *Giant Magnetoresistive(GMR) Spin-Valve* multilayer thin films.

$(25ANiFe/25ACu/25ANiFe^{A2}/25ACu)_{15}$

An Applied Field of 2 Oe orientated parallel to the EASY axis.
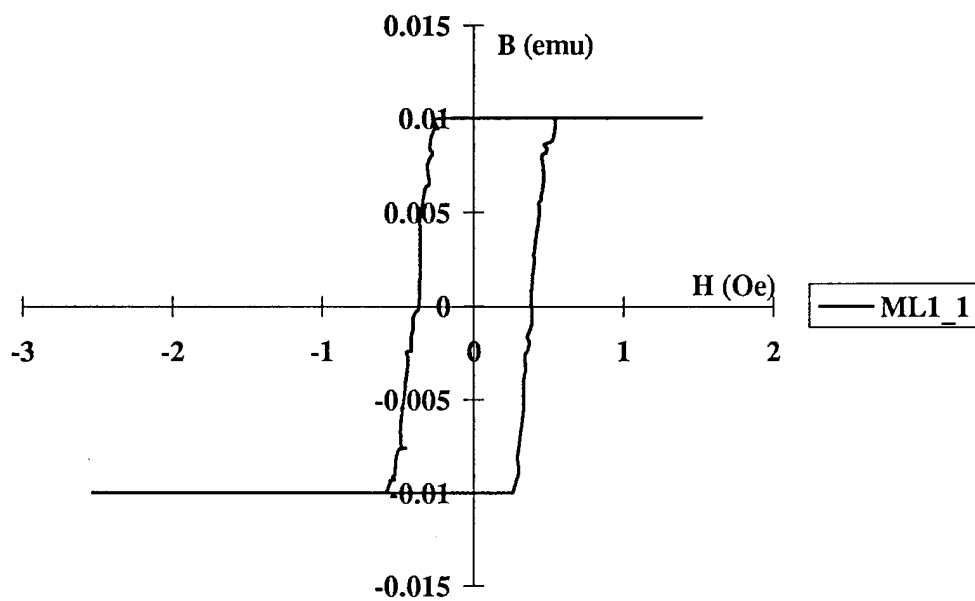
$(25ANiFe/25ACu/25ANiFe^{A2}/25ACu)_{15}$

An Applied Field of 50 Oe orientated parallel to the HARD axis.
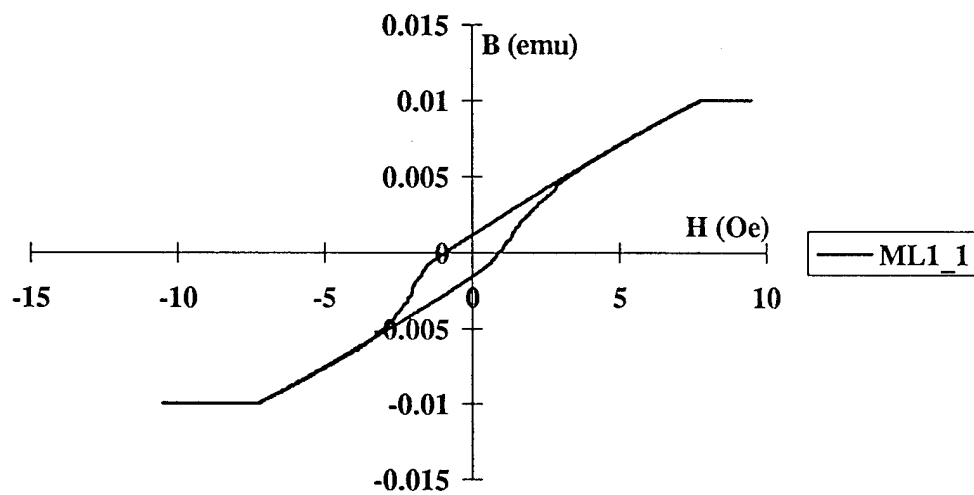
$(25ANiFe/40ACu/25ANiFe^{A2}/25ACu)_{15}$

An Applied Field of 3 Oe orientated parallel to the EASY axis.
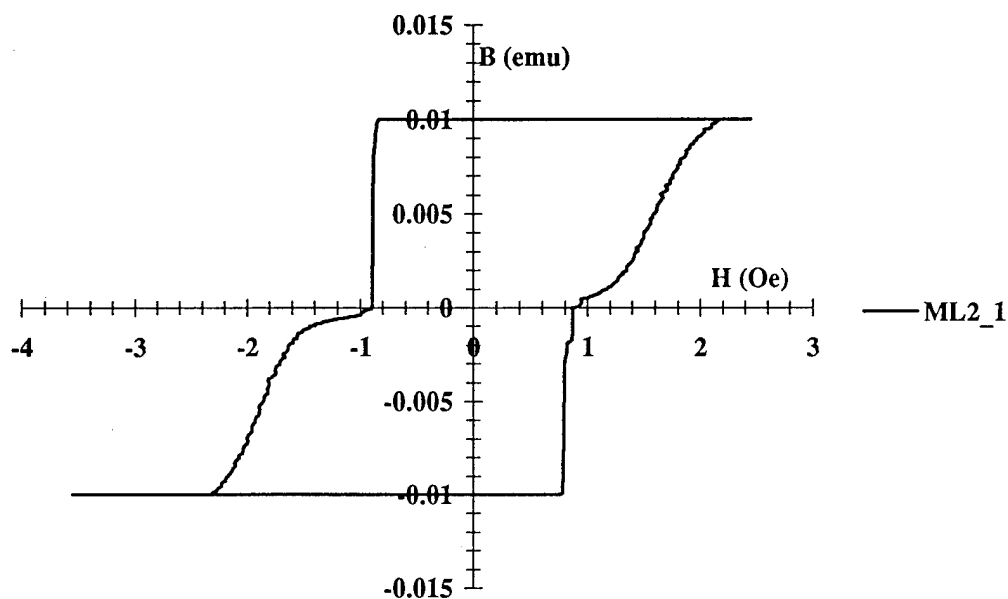
$(25ANiFe/40ACu/25ANiFe^{A2}/25ACu)_{15}$

An Applied Field of 50 Oe orientated parallel to the HARD axis.
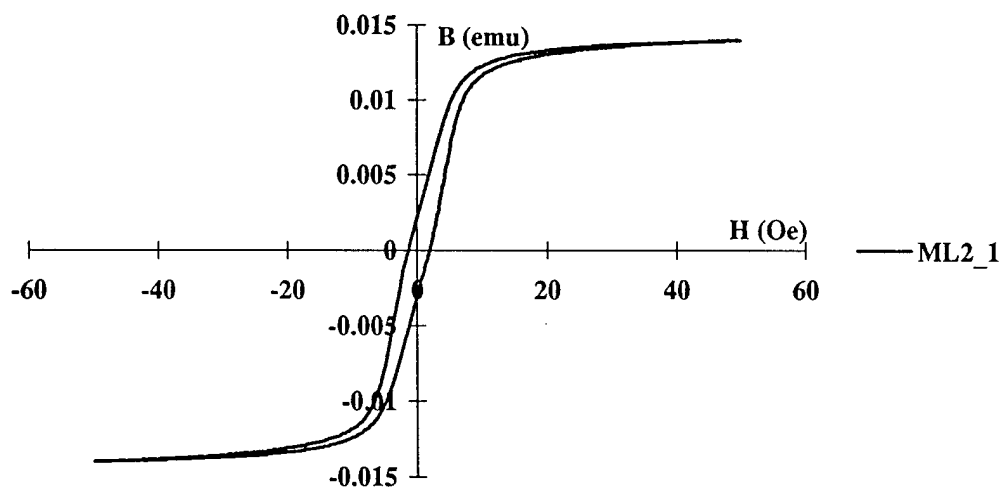
$(25ANiFe/55ACu/25ANiFe^{A2}/55ACu)_{15}$

An Applied Field of 50 Oe orientated parallel to the EASY axis.
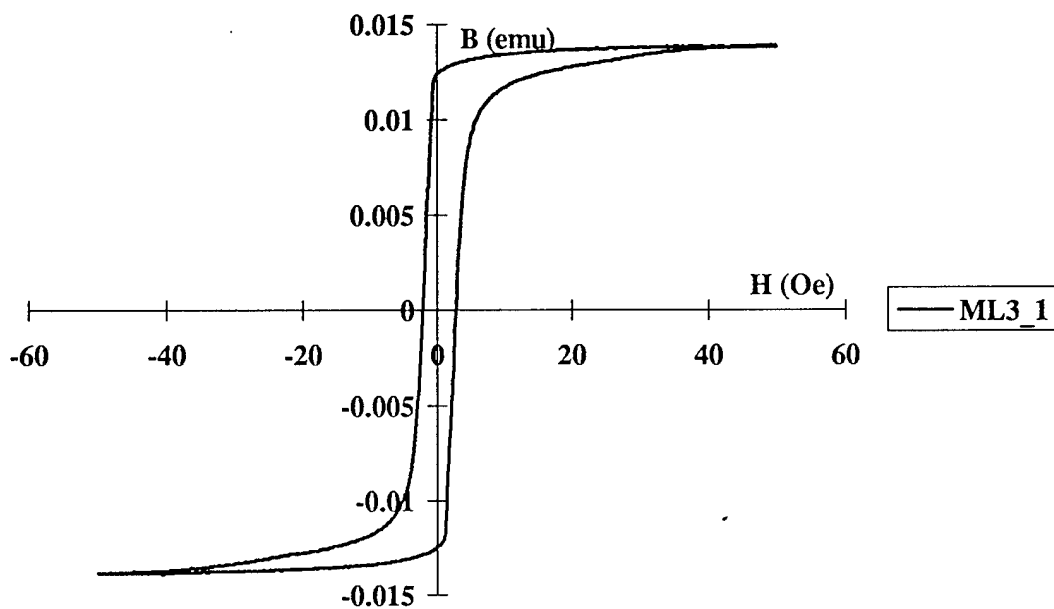
$(25ANiFe/55ACu/25ANiFe^{A2}/55ACu)_{15}$

An Applied Field of 10 Oe orientated parallel to the HARD axis.
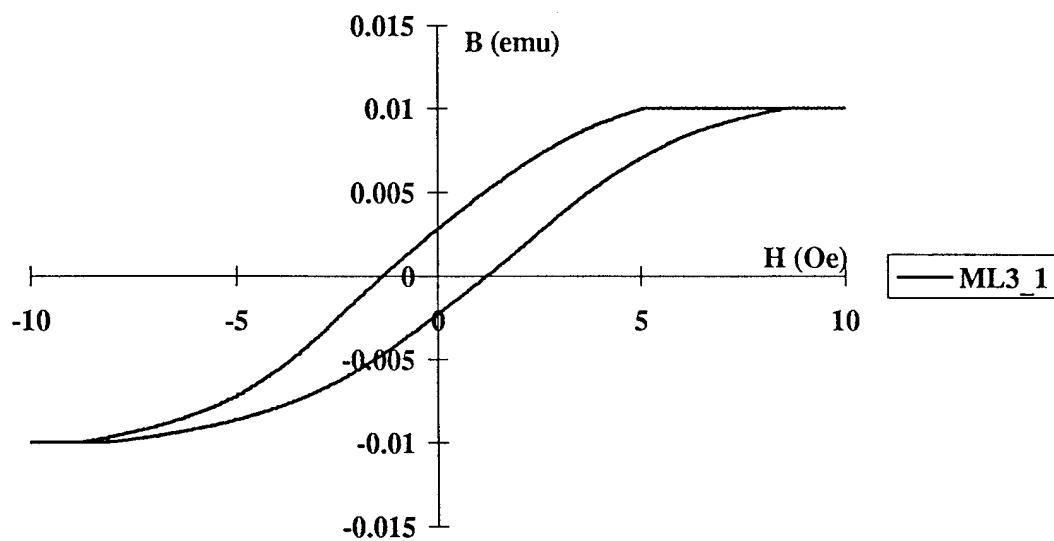
Giant Near-90° Coupling in
Epitaxial CoFe/Mn/CoFe Sandwich Structures

M.E. Filipkowski, Physics Dept., University of Arkansas,

J.J. Krebs and G.A. Prinz, Naval Research Laboratory,

and

C.J. Gutierrez, Physics Dept., Southwest Texas State University

ABSTRACT

Single crystal trilayer samples of CoFe/Mn/CoFe(001) have been prepared by molecular beam epitaxy and their magnetic properties measured by magnetometry and ferromagnetic resonance. The $Co_{75}Fe_{25}$ bcc alloy layers are roughly 100 Å thick and the bct Mn thicknesses range from 6 to 30 Å. Very strong near-90° coupling (up to 2.5 erg/cm^2) between the CoFe layers, with no evidence for 180° coupling, was found in all but the thickest Mn-layer samples. A detailed fit to the field dependence of the magnetization requires that the coupling energy have the algebraic form $F_c = C_+ (\phi_1 - \phi_2)^2 + C_- (\phi_1 - \phi_2 - \pi)^2$ suggested recently for the case when the interlayer itself is antiferromagnetic. The observed angular dependence of both the in-phase (acoustic) and out-of-phase (optical) FMR modes found in the strongly coupled trilayers can be described by this model.

PACS numbers: 75.70.-i, 75.70.Fr, 75.50.Rr, 76.50.+g

Vibrating sample magnetometer (VSM) and SQUID magnetometry, as well as 35 GHz FMR angular dependence, were carried out in plane on all samples to measure their magnetic properties.   All trilayers with t(Mn) < 30 Å exhibit evidence of coupling between the FM layers but, for clarity, we discuss only one sample (Sample A with t(Mn) = 11.2 Å) in detail.

The low-field VSM magnetization data for sample A are shown in Fig. 1. Note that they imply apparently easy <100> and hard <110> behavior in the (001) plane, exactly the reverse of the behavior of isolated CoFe films with the above composition.[5]   If, however, the Mn thickness is increased beyond 30 Å, the usual isolated film behavior is observed in both VSM and FMR.

The above results can be understood easily if the magnetizations M_1 and M_2 of the CoFe layers of sample A lie nearly perpendicular to one another in zero field, and along the expected in-plane <110> easy directions, so that the net magnetization $M = M_1 + M_2$ is along <100>, (see inset in Fig. 1). For strong nearly-90° coupling, as found here, M_1 and M_2 initially rotate as a rigid unit in an attempt to align M with H when a field H is applied along <110>, and they come together very slowly for H applied parallel to M along <100>. This type of behavior will be found as long as the coupling is large compared to both the in-plane anisotropy and -$M \cdot H$ energy density term, as explicit calculations show. The SQUID magnetization data for $H \parallel$ <110> are shown over a much more extended range in Fig. 2. Note that after the magnetization break near 1 kOe (when the rotation is complete), M continues to increase as the field causes M_1 and M_2 to come together, and M approaches saturation only slowly above 20 kOe.

The electronic basis for the coupling between ferromagnetic layers through an intervening metal film has been pointed out by several authors[1-3] to depend on the relative energy alignment of the spin-split bands in the ferromagnet with the paramagnetic bands in the interlayer. In the Fe/Cr/Fe system, which exhibits very strong coupling, the unsplit bands in paramagnetic Cr are nearly aligned with the minority bands in Fe.[2] Since both Fe and Cr are bcc, we felt that, if a new bcc layered system could be fabricated employing Co and Mn, respectively, there would be an opportunity to test this idea, since rigid band shifts would lead to a similar band alignment. The materials studied here (bcc CoFe alloy and bct Mn) provide a close approximation to the desired structure.

In this letter, we present the experimental results on this system, single crystal epitaxial sandwich structures of CoFe/Mn/CoFe, which exhibit the largest near-90° type coupling ever observed without any detectable bilinear coupling. The form of the coupling is consistent with a recent theoretical model based upon the intervening layer being an ordered antiferromagnet.[4]

A set of 15 trilayer samples were prepared by molecular beam epitaxy. The $Co_{75}Fe_{25}$ (001) alloy layers are all about 100 Å thick and were grown using methods described earlier.[5] They are bcc and exhibit RHEED patterns indicating excellent crystalline quality. The lattice constant for this composition alloy is a nearly perfect 2:1 match to that of the ZnSe/GaAs(001) sustrates used.[5] The Mn interlayer thicknesses range from 6 to 30 Å as determined by x-ray fluorescence. They are single crystal as shown by RHEED, while EXAFS measurements showed a bct structure with the tetragonal distortion along the growth direction.[6]

A quantitative fit to this (and the corresponding **H** || <100>) data requires one to write down the free energy per unit area,

$$F = F_c + F_a - \mathbf{H} \cdot (\mathbf{M}_1 + \mathbf{M}_2)t(CoFe), \qquad (1)$$

where F_c is the coupling energy/area, F_a is the corresponding anisotropy term, and $t(CoFe)$ is the thickness of a FeCo layer. Based on previous FMR measurements on isolated CoFe films,[5] we expect

$$F_a = t(CoFe) \sum_i \{K_1(\alpha_1^2\alpha_2^2 + \alpha_2^2\alpha_3^2 + \alpha_3^2\alpha_1^2) + K_u \cos^2(\phi-\phi_u)\}_i, \qquad (2)$$

with K_1/M and $|K_u/M|$ about -0.25 and 0.05 kOe, respectively. This permits one to determine the magnitude and form of the coupling term F_c.

Almost universally, the coupling which has been found experimentally in the many types of magnetic trilayer and superlattice samples studied to date has the form,

$$F_c = -2A_{12} \widehat{\mathbf{M}}_1 \cdot \widehat{\mathbf{M}}_2 - 2 B_{12}(\widehat{\mathbf{M}}_1 \cdot \widehat{\mathbf{M}}_2)^2, \qquad (3)$$

where A_{12} and B_{12} are the so-called bilinear and biquadratic coupling contants and $\widehat{\mathbf{M}}_i$ is a unit vector in the direction of $\mathbf{M}_i$. The values of A_{12} and B_{12} generally oscillate and decrease in magnitude as the interlayer thickness increases.[7] For dominant A_{12}, $\mathbf{M}_1$ and $\mathbf{M}_2$ anti-align for $A_{12} < 0$. However, if $|B_{12}| >> |A_{12}|$ and $B_{12} < 0$, the configuration $\mathbf{M}_1 \perp \mathbf{M}_2$ is favored. Both Fe/Cr/Fe and Fe/Al/Fe trilayers exhibit this 90° configuration for some interlayer thicknesses[8-11] but this is not the usual behavior for coupled magnetic films.

The dashed line in Fig. 2 a) and b) results from a least squares fit to the data of Fig. 2 via a minimization of F at each field yielding the following parameters: $2A_{12} = 0$ and $2B_{12} = -3.0$ erg/cm^2, $K_1/M = -0.31$ kOe and $K_u/M = 0.03$ kOe. Note that this calculation produces a rather poor fit above the break in the curve and shows an abrupt rather than a slow approach to saturation. This type of behavior is inherent to the A_{12}, B_{12}

coupling form of Eq. (3). We stress the fact that the $|A_{12}/B_{12}|$ ratio is quite small and this is found for all the coupled samples studied here. Such behavior is very unusual as is the large magnitude required for B_{12}. Previously, the largest value of $2B_{12}$ found is -0.3 erg/cm^2 for Fe/Al/Fe.[11] For the **H** || <100> magnetization data, this standard coupling form yields a similarly inadequate fit.

Recently, Slonczewski[4] has carried out a calculation of the type of coupling expected when the interlayer between the two FM layers is itself antiferromagnetically ordered. Due to competition between different areas in the interlayer which favor either alignment or anti-alignment of the FM layers, the coupling has the following anticipated form,

$$F_c = C_+ (\phi_1 - \phi_2)^2 + C_- (\phi_1 - \phi_2 - \pi)^2 , \tag{4}$$

where C_+ and C_- are the FM and AFM coupling constants and ϕ_i is the in-plane orientation angle of **M**$_i$. For $C_+ \approx C_-$, the favored configuration[4] has **M**$_1$ and **M**$_2$ nearly 90° apart. Note that Eq. (4) is algebraic rather than trigonometric (as Eq.(3) is) in the orientation angles.

The solid line in Fig. 2 is a fit to the data using the coupling form of Eq. (4) with the following least squares parameters: $C_+ = 0.95$ and $C_- = 1.07$ erg/cm^2, $K_1/M = -0.34$ kOe and $K_u/M = 0.03$ kOe. This is clearly a much improved representation of the magnetization data, especially in terms of the deficiencies noted earlier for the usual coupling form. Note that $C_+ \approx C_-$ as expected for the zero field orientation found. The fit for the **H** || <100> data using the same parameters (not shown) is similarly improved.

The above data thus offer strong evidence that Eq. (4) is the proper coupling for CoFe/Mn/CoFe and, furthermore, imply that the Mn interlayer is antiferromagnetically ordered, at least for small t(Mn). Recent soft x-

ray magnetic circular dichroism and polarized neutron diffraction measurements on a superlattice of CoFe/Mn, with t(Mn) chosen for very strong coupling, support the existence of Mn moments[12] as well as the near-90° orientation of adjacent CoFe layer moments.[13]

Finally, we briefly consider the FMR modes found in the strongly coupled trilayers. The angular dependence of the two modes found is shown via the points in Fig. 3. The high field mode is identified as an in-phase (acoustic) mode and the low field one as out-of-phase (optical) by means of their distinct polarization behavior. The in-phase mode is strong when the microwave magnetic field $\mathbf{h_1} \perp \mathbf{H}$ and the out-of-phase mode is when $\mathbf{h_1} \parallel \mathbf{H}$. An attempt to fit the angular dependence of these modes was made using the same energy density techniques described earlier for Fe/Cr/Fe coupled trilayers.[14] We note that the demagnetizing term $- 2\pi(M_{1z}^2 + M_{2z}^2)t(CoFe)$ must be appended to the areal energy density F for this calculation.

Using the standard (Eq.(3)) coupling term, one can not obtain even a qualitatively acceptable fit. On the other hand, using Eq. (4), one obtains the qualitatively correct fits to the average field and the angular dependence of the two modes as shown by the solid lines in Fig. 3. This fit has an extra coupling term $C_z(\theta_1 - \theta_2)^2$ added to allow for a different coupling along the tetragonal distortion direction of the Mn layer. Although the distinctive qualitative behavior of the FMR modes is well reproduced, we do not consider the fit adequate nor can we justify the small C_z/C_+ ratio of 0.67 needed. Rather, we suggest that the model used is over-simplified for treating the FMR modes, in that it assumes one can treat the FM layers as rigid entities characterized by unique magnetization angles and that the Mn layer can be replaced by simple interface

coupling contants. It seems clear that a more sophisticated model explicitly dealing with the change in magnetic moment direction throughout the Mn layer and into both alloy films will be needed for a precise treatment of the behavior of the FMR modes.

We believe that this system, which employs metastable bct Mn to couple the ferromagnetic layers, repesents a new departure for studies of coupled layers, and the strong near-90° coupling at room temperature may prove useful for technological applications. The existence of this anti-ferromagnetically mediated coupling in CoFe/Mn suggests that the Fe/Cr system should be re-examined with this in mind. This work was supported by the Office of Naval Research.

REFERENCES

1. D.M. Edwards, J. Mathon, R.B. Muniz, and M.S. Phan, J. Phys. Condens. Matter **3**, 4941 (1991).

2. K.B. Hathaway and J.R. Cullen, J. Magn. Magn. Mater. **104-107**,1840, (1992).

3. R.P. Erickson, K.B. Hathaway and J.R. Cullen, Phys. Rev. B **47**, 2626 (1993).

4. J.C. Slonczewski, J. Magn. Magn. Mater. (to be published).

5. C.J. Gutierrez, J.J.Krebs, and G.A. Prinz, Appl. Phys. Lett. **61**, 2476 (1992). Note that the K_1 values listed need to be multiplied by a factor of 10^5.

6. Y.U. Idzerda, private communication

7. B. Heinrich and J.F. Cochran, Adv. in Phys. **42**, 523 (1992); J. C. Slonczewski, Phys. Rev. Lett. **67**, 3172 (1991).

8. M. Ruhrig, R. Schafer, A. Hubert, R. Mosler, J.S. Wolf, S. Demokritov and P. Grünberg, Phys. Stat. Sol. (a) **125**, 635 (1991).

9. J. Unguris, R.J. Celotta, and D.T. Pierce, Phys. Rev. Lett. **67**, 140 (1991).

10. A. Fuss, S. Demokritov, P. Grünberg, and W. Zinn, J. Magn. Magn. Mater. **103**, L221 (1992).

11. C.J. Gutierrez, J.J.Krebs, M.E. Filipkowski, and G.A. Prinz, J. Magn. Magn. Mater. **116**, L305 (1992).

12. V. Chakarian, Y.U. Idzerda, H.J. Lin, C.J. Gutierrez, G.A. Prinz, G. Meigs, and C.T. Chen, (to be published).

13. J.A Borchers, private communication

14. J.J.Krebs, P. Lubitz, A. Chaiken and G.A. Prinz, J. Appl. Phys. **67**, 5920 (1990); Phys. Rev. Lett. **63**, 1643 (1989).

FIGURE CAPTIONS

Fig. 1   Magnetic moment vs magnetic field data for a CoFe/Mn/ CoFe(001) trilayer sample with t(Mn) = 11.2 Å (sample A).   The in plane magnetic field is applied along the directions indicated. Inset: Moment directions in zero field.

Fig. 2   Field dependence of the magnetization of sample A over an extended field range with $\mathbf{H} \parallel$ <110>.   Inset: Details of the low field region.   The data are indicated by the open circles while fits based on the coupling expressions of Eq.(3) and Eq.(4) in the text are shown by the dashed and solid curves, respectively.

Fig. 3   The in-plane angular dependence of the in-phase and out-of-phase FMR mode positions for sample A.   The open dots are the experimental data and the thin line is a guide to the eye.   The heavy solid line fit with C_+ (= C_-) and C_z equal, respectively, to 1.01 and 0.67 erg/cm^2 is discussed in the text.
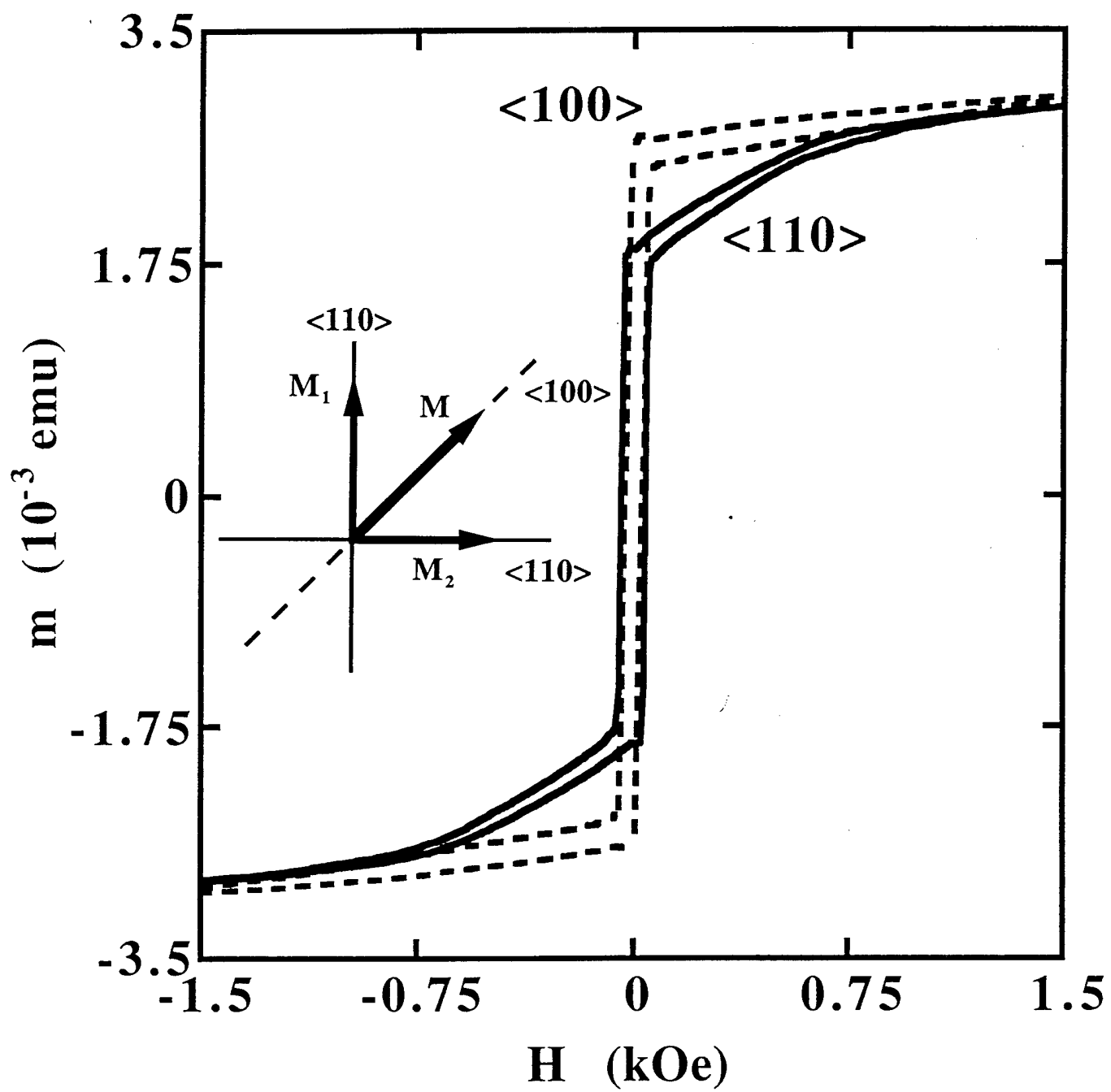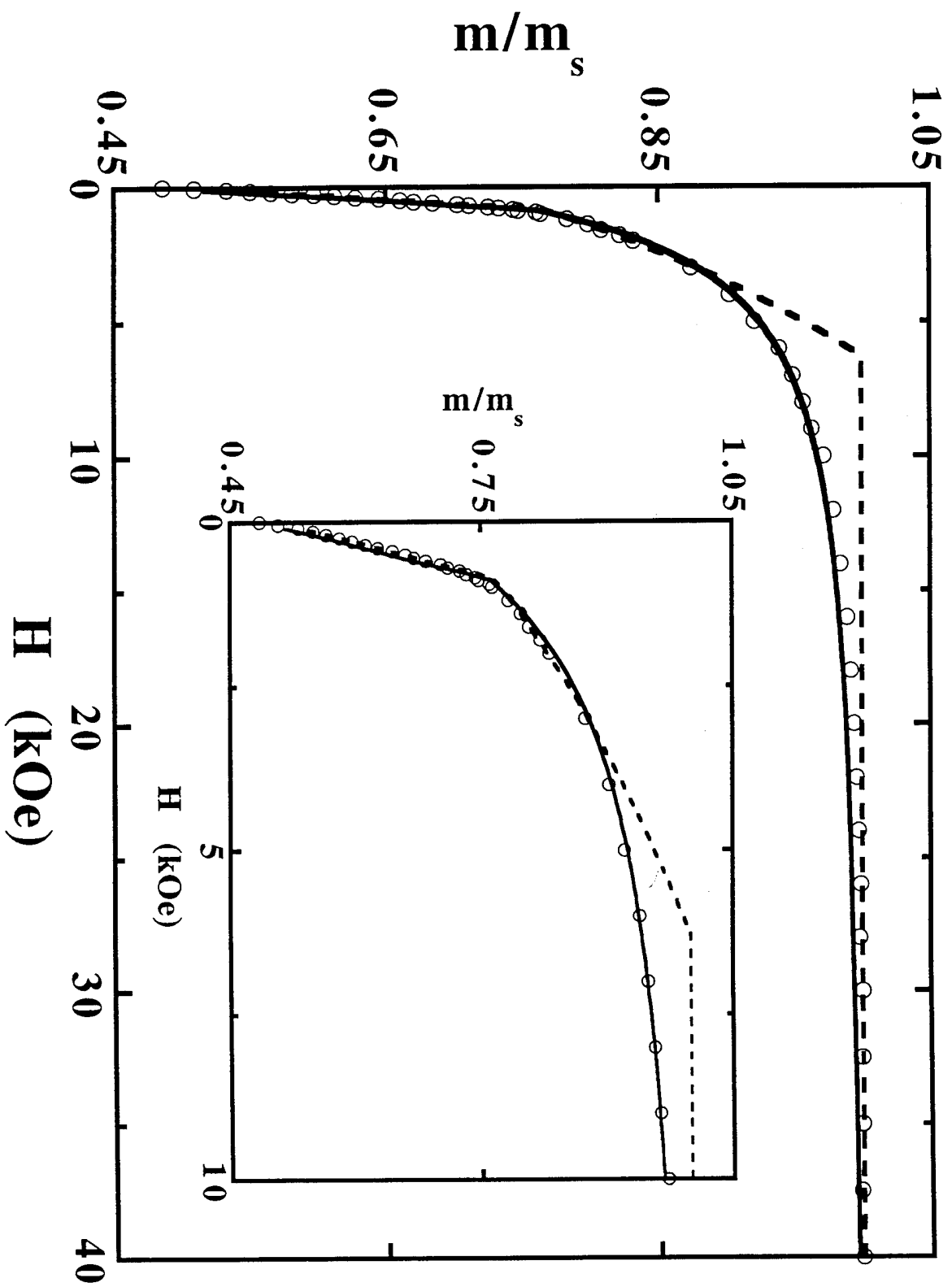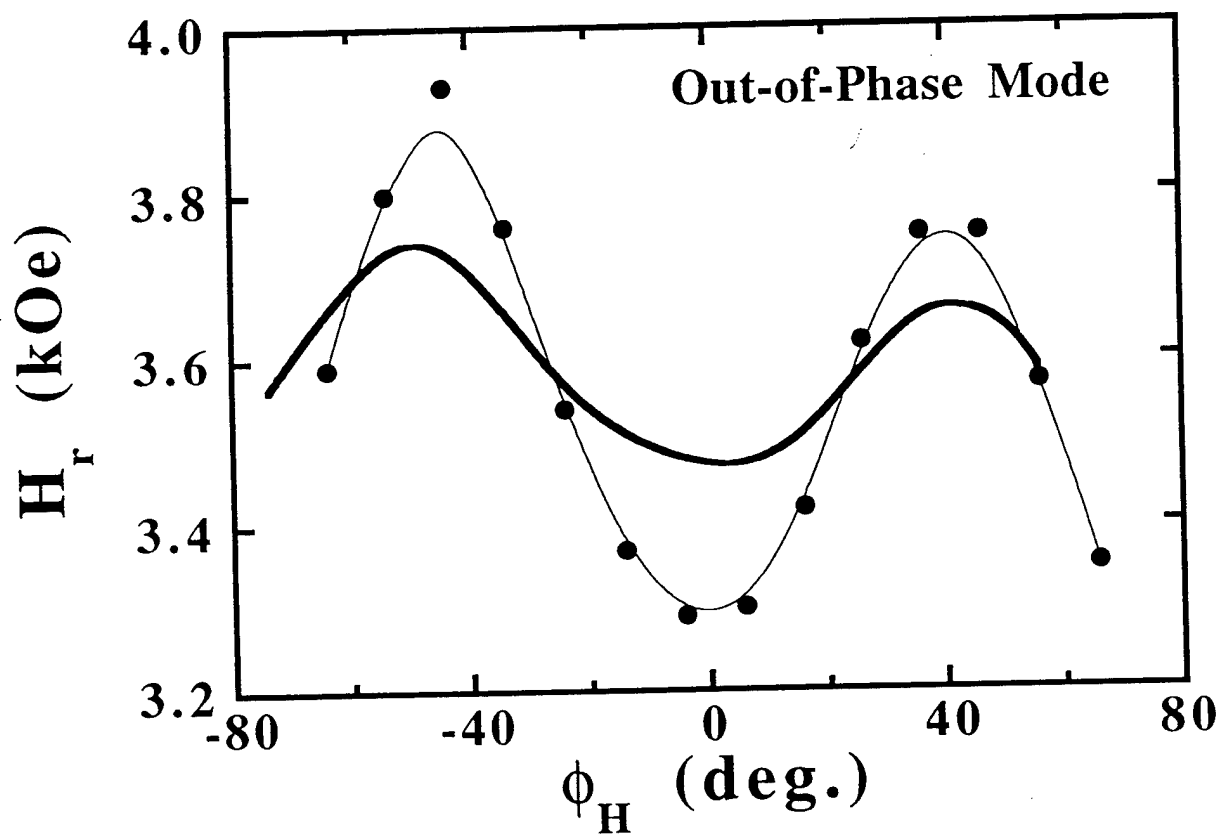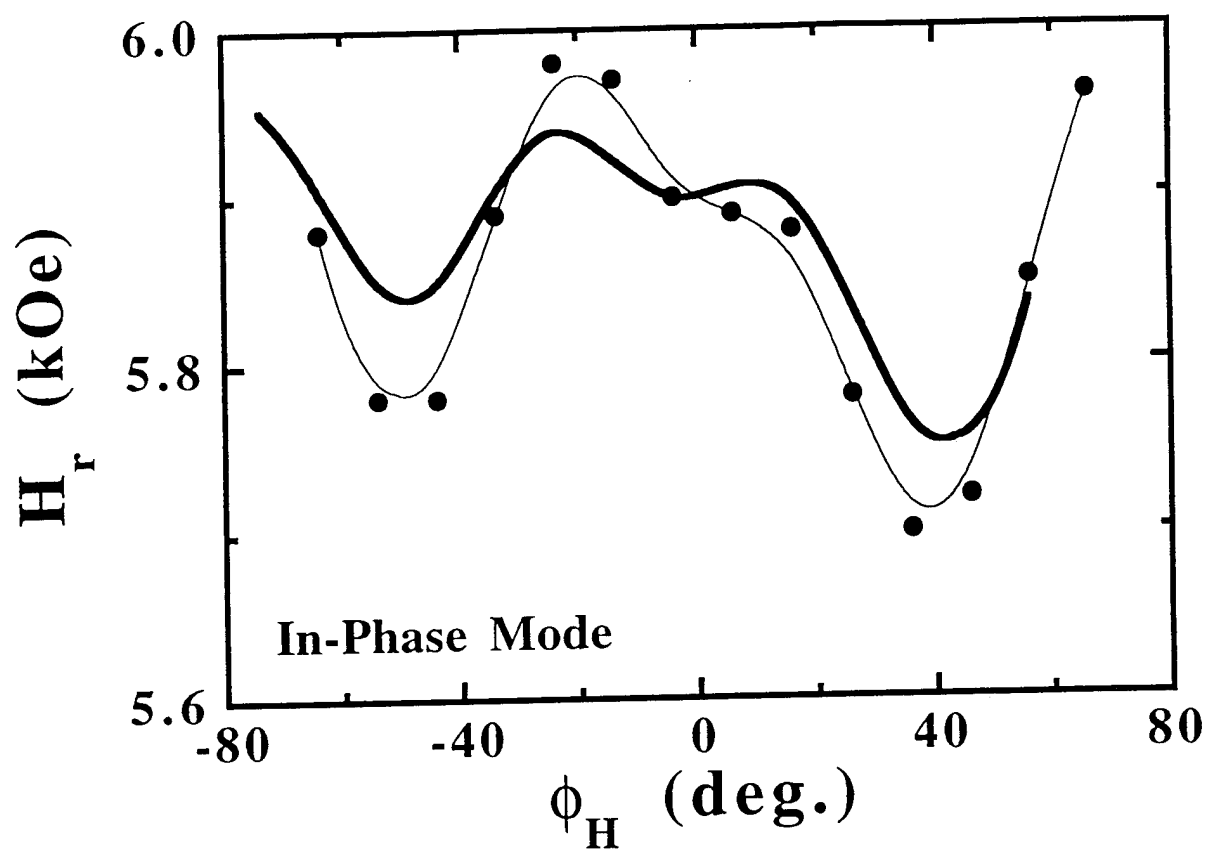
Fig. 1

Fig. 2

In-Phase Mode

Out-of-Phase Mode

Fig. 3

ELEMENT SPECIFIC VECTOR MAGNETOMETRY (ESVM) VIA SOFT X-RAY MAGNETIC CIRCULAR DICHROISM

V. CHAKARIAN,[1]† H.-J. LIN,[2]‡ Y.U. IDZERDA,[1] E.E. CHABAN,[2] G. MEIGS,[2] J.-H. PARK,[2] C.J. GUTIERREZ,[1] G.A. PRINZ,[1] AND C.T. CHEN[2]

[1] *Naval Research Laboratory, Code 6345, Washington, DC 20375 USA*
[2] *AT&T Bell Laboratories, 600 Mountain Ave., Murray Hill, NJ 07974 USA*

ABSTRACT

Soft X-Ray Magnetic circular dichroism (SX-MCD) can be used to obtain element-specific magnetic hysteresis curves and to elucidate the two- and three-dimensional magnetization reversal processes for each constituent magnetic element of a heteromagnetic system. As a demonstration, two systems which exhibit in-plane magnetization reversal are studied: a thin Fe (100) single-crystal film and a $Fe_{1-x}Co_x/Mn/Fe_{1-x}Co_x$ trilayer. The results for both systems show that the magnetic moment vector reverses via a combination of coherent rotation toward the nearest in-plane magnetically easy axis followed by the formation of orthogonal <100> domains which rapidly sweep across the sample. In the case of the trilayer,the moment reversal process is significantly more complex due to a strong ~90° coupling between the magnetic moments of the two FeCo layers. By using element-specific vector magnetometry (ESVM), the details of this reversal process are revealed. Furthermore, the results of the SX-MCD for Mn show that Mn possesses a ferromagnetically aligned net magnetic moment which depicts a 2D magnetization behavior different than that for either Fe or Co.

INTRODUCTION

For magnetic materials the magnetization **M** is a crucial vector quantity defining their properties.[1] The direction in which **M** points and how this direction changes as a function of the applied magnetic field is a central issue for many technological application of magnetic materials. Magnetization reversal in thin ferromagnetic films has been studied via a wide variety of methods which includes vibrating sample magnetometry, magnetization loopers, magneto-optic Kerr effect (MOKE), magnetoresistance, superconducting quantum interference device susceptometry and Lorentz electron microscopy.[2] These conventional methods are often used to determine the magnitude and/or the orientation of only a single component of the magnetic moment vector (typically parallel to the applied magnetic field). In the case of MOKE, by using longitudinal Kerr effect one can obtain the two in-plane orthogonal components of the magnetization.[3] Nevertheless, in the case of heteromagnetic systems, none of the aforementioned methods discriminate among the various constituent elements of the magnetic material studied, nor do they allow the determination of the magnetization change in three dimensions. Therefore, most previous studies involving magnetization reversal in mono- and heteromagnetic systems provide valuable but limited and incomplete information regarding the magnetization process.

In this work, the use of soft X-ray magnetic circular dichroism (SX-MCD) as a unique and powerful tool for element-specific, 2D and 3D vector magnetometry of mono- and heteromagnetic thin films and multilayers is demonstrated. SX-MCD is an element-specific magnetic spectroscopic tool in which the difference in the absorption of left- and right-circularly polarized photons are measured at the absorption edges of the constituent elements. This difference in absorption cross-sections (normalized to the total absorption cross-section) is proportional to the average magnetic moment at a given atomic site. An alternate, and equivalent, method for measuring SX-MCD is to reverse the applied magnetic field direction while keeping the

---

† *Mailing address:*   NSLS 725A-U4B, Brookhaven National Lab, Upton, NY 11973
‡ *Present address:*   Synchrotron Radiation Research Center, Hsin-Chu Science-Based Industrial Park, Hsin-Chu, Taiwan, R.O.C.

polarization of the incident photon beam fixed.[4] This latter method permits one to obtain element-specific magnetic hysteresis curves by monitoring the peak height of a given elemental white line, e.g. the L_3 white line of $3d$ transition metals, as a function of the applied magnetic field.[5]

As a demonstration of the technique, the experiments are first performed on a relatively simple and well studied system: Fe (001) thin film grown on ZnSe (001) substrate. The power of the technique is then demonstrated by determining the magnetization reversal within the $Fe_{0.3}Co_{0.7}$ and Mn layers *separately* in a $Fe_{0.3}Co_{0.7}/Mn/Fe_{0.3}Co_{0.7}$ trilayer system in which the adjacent $Fe_{0.3}Co_{0.7}$ layers are oriented with respect to one another by a coupling angle.

EXPERIMENTAL PROCEDURES

The experiments were conducted at the AT&T Bell Laboratories "Dragon" beamline located at the National Synchrotron Light Source, Brookhaven National Laboratory.[6-8] The experimental setup of the beamline for the MCD[4] and element-specific magnetic hysteresis (ESMH) curve measurements have been described previously[5] Briefly, ESMH curves were recorded by monitoring the L_3 white line partial fluorescence yield intensity of the relevant elements with a high-sensitivity, seven-element solid-state germanium detector as a function of the applied field. The field intensity was calibrated by comparing the SX-MCD hysteresis loops to the VSM loops obtained previously.

A special UHV compatible electromagnet assembly, capable of reaching ~3 kG, has been designed and constructed for these measurements which allows one to change the magnetization direction relative to the incident photon direction via either independent or concerted rotation of the sample and the magnet.[9] Two samples, grown by molecular beam epitaxy (MBE), were used for these experiments: A 30 Å Fe (001) single-crystal thin film and a $Fe_{0.3}Co_{0.7}$(106 Å)/Mn(8.7 Å) /$Fe_{0.3}Co_{0.7}$(106 Å) trilayer. Both samples were grown on a ZnSe (001) buffer layer grown on GaAs (001) substrate in an MBE chamber. The quality of the films as well as growth direction were monitored via in-situ reflection high energy electron diffraction measurements.

VECTOR MAGNETOMETRY METHOD

The magnetization vector, $\mathbf{M}$, can be expressed in 3D as $\mathbf{M} = M_x \hat{x} + M_y \hat{y} + M_z \hat{z}$. The measured hysteresis curves are proportional to $\mathbf{k_i} \cdot \mathbf{M}$, where $\mathbf{k_i}$ is the photon momentum (incident photon beam direction). The direction of the magnetization vector relative to the incident photon beam direction can be varied by simply rotating the sample-magnet assembly relative to the photon direction. An illustration of this process is shown in Fig. 1 in which the x-direction is defined along the applied field, $\mathbf{H}$. The azimuthal rotation of the magnetization direction successively by 90° results in a photon momenta to be along one of the $\mathbf{k_i}$ (i = 1, 2, 3, 4) shown in the figure. The individual components of the magnetization vector can then be obtained uniquely by forming arithmetic sums and differences of the measured hysteresis curves as follows:

$$\mathbf{k_1} \cdot \mathbf{M} - \mathbf{k_3} \cdot \mathbf{M} = 2\,p \sin \vartheta\; M_x \qquad (1a)$$
$$\mathbf{k_2} \cdot \mathbf{M} - \mathbf{k_4} \cdot \mathbf{M} = -2\,p \sin \vartheta\; M_y \qquad (1b)$$
$$\mathbf{k_1} \cdot \mathbf{M} + \mathbf{k_3} \cdot \mathbf{M} = \mathbf{k_2} \cdot \mathbf{M} + \mathbf{k_4} \cdot \mathbf{M} = -2\,p \cos \vartheta\; M_z \qquad (1c)$$

where ϑ is the angle between the photon momenta and the surface normal and p is the degree of circular polarization of the incident photon beam and has a value between -1 and 1. In principle, only three measurements are needed to uniquely determine $\mathbf{M}$. The four rotation method described here is for arithmetic simplicity and provides an internal consistency check.

Once M_x, M_y and M_z are determined, a 3D view of the moment reversal can then be constructed. Note that, for thin films that display only in-plane magnetizations, as it was the case for the systems described in the present work, $M_z = 0$ so that measurements along $\mathbf{k_1}$ and $\mathbf{k_2}$ (or alternately, $\mathbf{k_3}$ and $\mathbf{k_4}$) are sufficient for obtaining M_x and M_y. For this work, hysteresis curves were also collected along a direction 45° to the x-z and y-z planes which yields $(M_x + M_y)/\sqrt{2}$ and serves as an internal normalization. The lack of an M_z component was confirmed via the observation of a null MCD signal for photon beam incident normal to the film plane.

Fig. 1. Schematic diagram depicting the experimental setup. The sample-magnet assembly is azimuthally rotated with respect to the photon beam direction in increments of 90°. A set of four such measurements is sufficient to uniquely determine the orthogonal components of the magnetic moment vector, M.
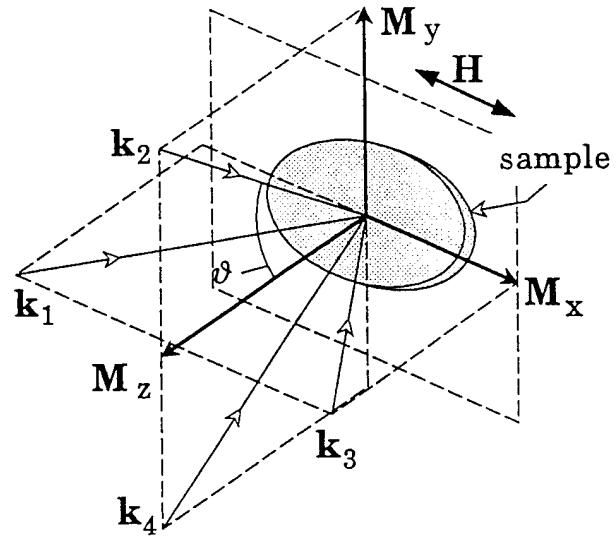
RESULTS AND DISCUSSION
Fe (001) film

Magnetic hysteresis behavior of the *net* magnetic moment along directions parallel (M_x) and perpendicular (M_y) to the applied field direction are shown on the left panel of Fig. 2. The magnetization curves are scaled so that the saturation states are at values of ± 1 in intensity. The arrows in the figure indicate the direction of the magnetization change for each loop. Also shown in the figure (inset) is a parametric representation of the M_x and M_y curves, which shows the two-dimensional (2D) rotation of the net magnetization vector. A more instructive representation of the same data is a 3D view of the two dimensional rotation of M and is shown on the right panel of Fig. 2. In this view, the M_x vs. H, M_y vs. H and M_x vs. M_y curves are all visible and the magnetization behavior of the film is revealed more clearly.
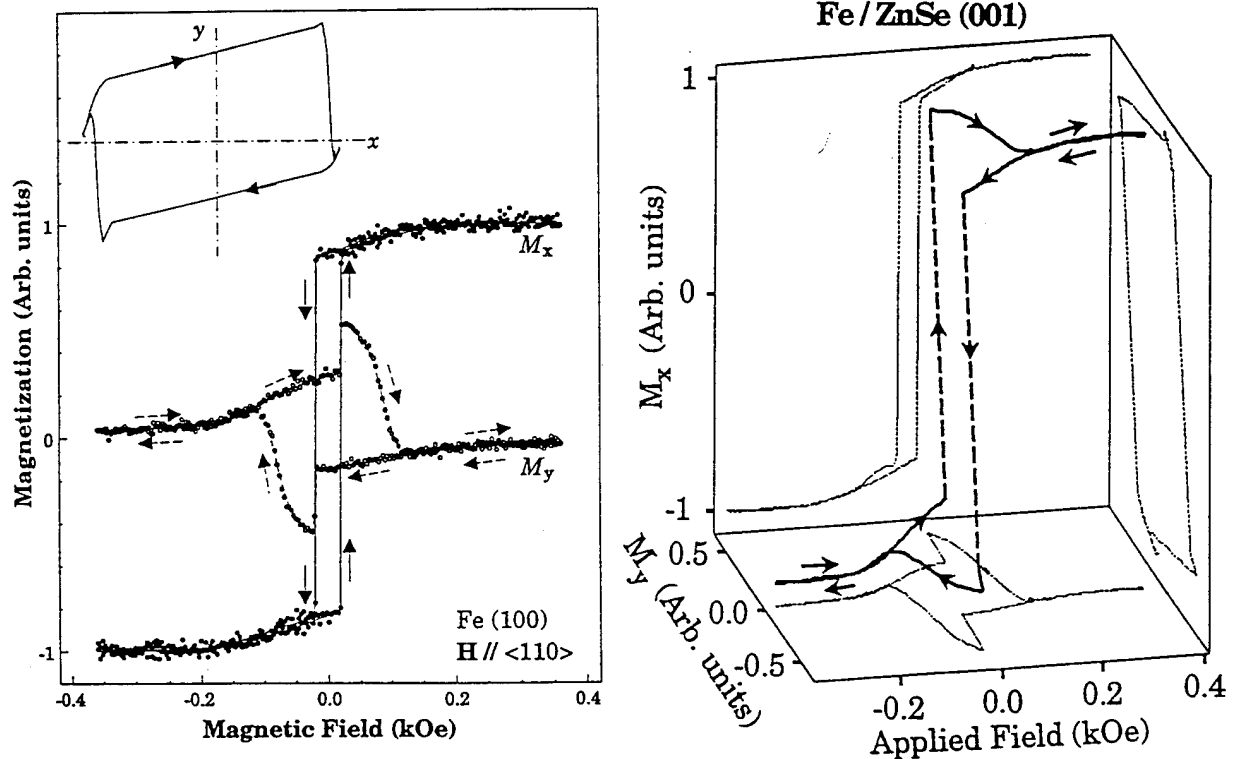

Fig. 2. (Left panel) M_x and M_y components of M for the Fe (001) thin film. Inset: 2D parametric plot of M_x vs. M_y. (Right panel) A 3D view of M in which the projections on the back, bottom and right planes are the M_x, M_y and M_x vs. M_y curves, respectively.

The vector nature of the magnetization reversal and the presence of a coherent rotation of **M** are clearly evident in these panels. As the magnetic field is varied from about -200 Oe to +20 Oe, the amplitude of M_y gradually increases as the amplitude of the M_x decreases by a comparable amount (similarly in the reverse direction). A more detailed analysis of this hysteresis behavior reveals[9] that the magnetization reversal process involves a coherent rotation of **M** toward the in-plane <100> easy axes followed by domain formation just prior to moment flipping. The irreversible jumps observed are the result of rapid domain dynamics across the sample immediately above the critical field. The moment reversal process is completed by the coalescence of these domains and a coherent rotation of **M** into alignment along the applied field.

$Fe_{0.3}Co_{0.7}/Mn/Fe_{0.3}Co_{0.7}$

In order to demonstrate the *element-specific* nature of the technique, magnetic hysteresis curves of a $Fe_{0.3}Co_{0.7}/Mn/Fe_{0.3}Co_{0.7}$ trilayer system are measured. The results of magnetometry, ferromagnetic resonance, and neutron scattering studies of this system suggest a strong coupling between the FeCo layers such that the magnetic moment vectors, M_i (i=1, 2), of the two layers are oriented with respect to one another by a coupling angle,[10] requiring a very large magnetic field to overcome this coupling between the FeCo layers (15-20 kG).

In Fig. 3, the relative M_x and M_y magnetization curves for Fe (left) and Mn (right) are shown (the Co magnetization curves are identical to that of Fe). Note that, due to large probing depth of the fluorescence yield measurements, the magnetization curves shown in the figure represent the rotation of the *average* moment, <**M**>, and not the individual moments of the two FeCo films. The arrows indicate increasing and decreasing magnetic field for the M_x (solid arrows) and M_y (dashed arrows) magnetization curves. An inspection of the M_x and M_y curves shows that the behavior of Mn moment is seemingly more complicated than that of either Fe or Co. One of the major conclusions of this work is that Mn has a net moment in this trilayer structure. Furthermore, a comparison of the switching fields for Fe and Mn moments indicates that Mn moment is coupled strongly to the enclosing FeCo layers. It is important to emphasize that SX-MCD is the only method that allows the determination of the Mn moment.
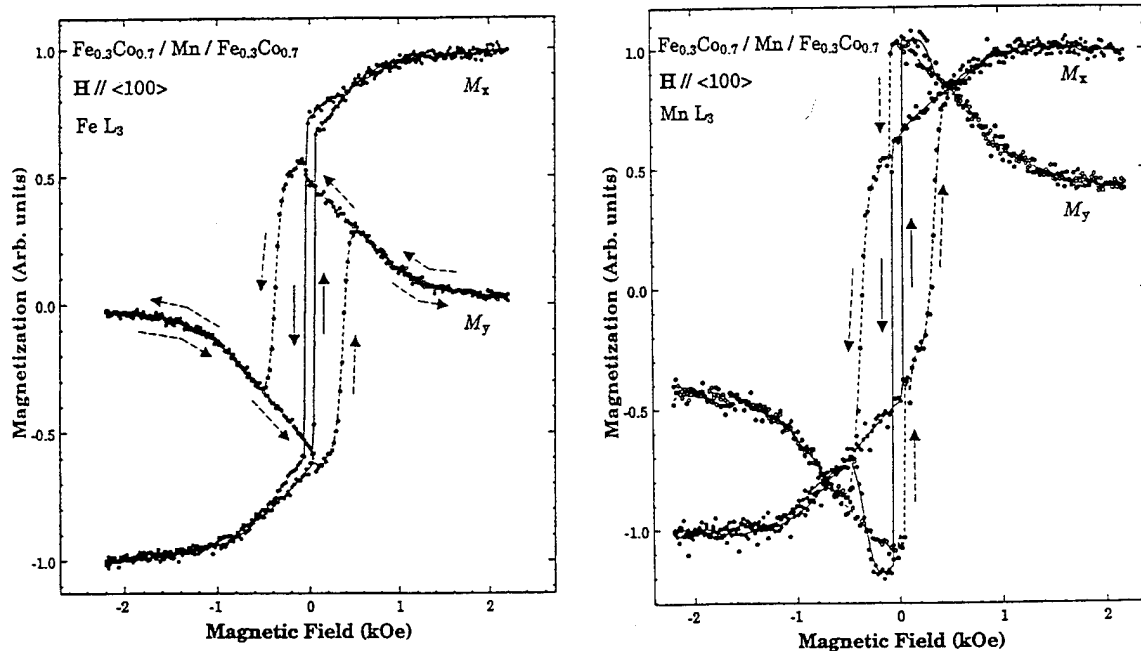

Fig. 3. M_x (solid) and M_y (dashed) components of average Fe moment (left panel) and Mn (right panel) in the $Fe_{0.3}Co_{0.7}/Mn/Fe_{0.3}Co_{0.7}$ trilayer.

In Fig. 4, a 2D parametric representations of <M> for Fe and Mn (from Fig. 3) of this system are shown. Also shown in the figure are the principal crystallographic directions present in the (001) plane. As the magnetic field is scanned from +2.2 kOe to −2.2 kOe <M> traverses the upper half of the loop in the counter-clockwise (ccw) direction. Along the opposite magnetization direction, the average M traverses the lower half of the loop. This parameterization indicates that the complicated Mn hysteretic behavior of Fig. 3 is simply the result of an average Mn moment oriented 25° with respect to the average Fe and Co moments. As the moments of the FeCo layers rotate in the plane of the film, the associated Mn moment maintains this 25° angle.

The 2D parametric loop of <M> for Fe (Co) can be used to model the rotation of the magnetic moments of each FeCo layer, M_i (i = 1, 2), as a function of the applied field.[9] Briefly, the behavior of M_1 and M_2 can be described by a combination of a coherent rotation and rapid domain wall motion across the sample. In this model it is assumed that at these fields the coupling between the two FeCo layers persists throughout the entire magnetization process and that both layers contribute equally to <M>. At saturation, the moments M_i of both FeCo films are along the two in-plane <110> directions such that M_1 and M_2 remain perpendicular to each other. As the intensity of the field is reduced, both M_1 and M_2 rotate ccw toward the two in-plane <100> directions. At the first critical fields of $H_c = \pm55$ Oe, domain wall motion within each layer results in a rapid and coherent 90° rotation of both film moments in such a way as to locally preserve the coupling between the films. This is followed by subsequently slower domain dynamics representative of an additional 90° coherent rotation, ending by the coalescence of the domains within each layer. As the field is swept in the opposite direction, M_1 and M_2 continue this ccw rotational scheme. It is important to note that reversing the applied field direction does not result in the opposite magnetization reversal process.
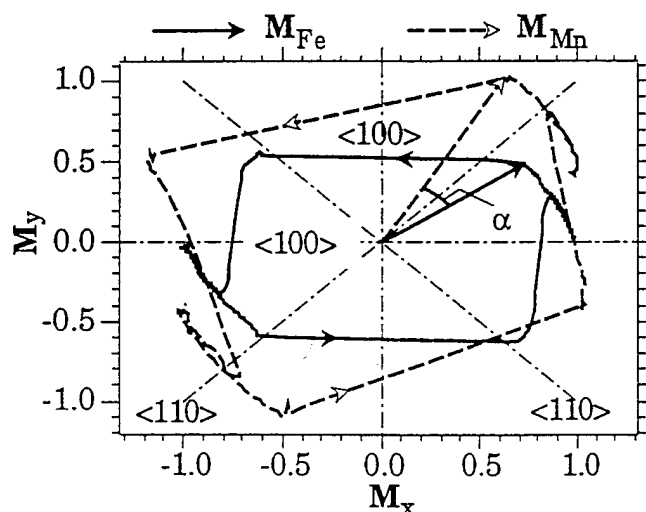

Fig. 4. 2D parametric representations of net Fe (solid) and Mn (dashed) magnetization curves (Co magnetization is similar to that of Fe). At any given field, the average Mn moment is oriented at an angle α with respect to the Fe and Co average moments.

CONLUSION

It has been demonstrated that element-specific magnetic hysteresis curves obtained via SX-MCD can be used to construct a vector representation of magnetic moment reversal in a thin film. The components of the magnetization vector M parallel and perpendicular to the applied field direction, M_x and M_y, respectively, are measured by rotating the sample/magnet assembly by 90° with respect to the incident photon direction. These M_x and M_y curves are then used to construct a 2D representation of M.

Two systems, with substantially different magnetization behavior have been studied. The first system, an Fe (100) thin film grown on GaAs (100), was magnetized along a direction nearly parallel to one of the in-plane <110> axes. The second system, a $Fe_{0.3}Co_{0.7}/Mn/Fe_{0.3}Co_{0.7}$ trilayer grown on GaAs (100), was magnetized along the <100> direction. The results for both systems indicate that, the magnetization reversal process is a combination of coherent rotation and sudden flipping of M into alignment with one of the in plane <100> axes.

ACKNOWLEDGMENTS

REFERENCES

1. S. Chikazumi, *Physics of Magnetism* (Krieger, Malabar, Florida, 1964).
2. L. M. Falicov, D. T. Pierce, S. D. Bader, R. Gronsky, K. B. Hathaway, H. J. Hopster, D. N. Lambeth, S. S. P. Parkin, G. Prinz, M. Salamon, I. K. Schuller and R. H. Victora, J. Mater. Res. **5**, 1299 (1990), and references therein.
3. C. Daboo, J. A. C. Bland, R. J. Hicken, A. J. R. Ives and M. J. Baird, Phys. Rev. B **47**, 11852 (1993).
4. C. T. Chen, F. Sette, Y. Ma and S. Modesti, Phys. Rev. B **42**, 7262 (1990).
5. C. T. Chen, Y. U. Idzerda, H.-J. Lin, G. Meigs, A. Chaiken, G. A. Prinz and G. H. Ho, Phys. Rev. B **48**, 642 (1993).
6. C. T. Chen, Nucl. Instrum. Methods Phys. Res. A **256**, 595 (1987).
7. C. T. Chen and F. Sette, Rev. Sci. Instrum. **60**, 1616 (1989).
8. C. T. Chen, Rev. Sci. Instrum. **63**, 1229 (1992).
9. V. Chakarian, H.-J. Lin, Y. U. Idzerda, G. Meigs, E. Chaban, J.-H. Park, G. A. Prinz and C. T. Chen, to be published.
10. M. E. Filipkowski, private communication.